Methods for localizing and quantifying radionuclide sources and deposition using in situ gamma spectrometry

Critical review of the peak-to-valley method based on experimental studies and applications in Georgia and Japan

Östlund, Karl

2017

Document Version:
Publisher's PDF, also known as Version of record

Methods of localizing and quantifying radionuclide sources and deposition using in situ gamma spectrometry

Critical review of the peak-to-valley method based on experimental studies and applications in Georgia and Japan

KARL ÖSTLUND
DEPARTMENT OF TRANSLATIONAL MEDICINE | LUND UNIVERSITY 2017

Methods of localizing and quantifying radionuclide sources and deposition using *in situ* gamma spectrometry

Methods for localizing and quantifying radionuclide sources and deposition using *in situ* gamma spectrometry

Critical review of the peak-to-valley method based on experimental studies and applications in Georgia and Japan

Karl Östlund

LUND
UNIVERSITY

DOCTORAL DISSERTATION
By due permission of the Faculty of Science, Lund University, Sweden.
To be defended at room 2005-7, Inga-Marie Nilssons gata 49,
1 of June 2017 at 09:00.

Faculty opponent
Professor David C.W. Saunders,
University of Glasgow, Scotland

Organization LUND UNIVERSITY	Document name DOCTORAL DISSERTATION
	Date of issue 2017-06-01
Author(s) Karl Östlund	Sponsoring organization: Strålsäkerhetsmyndigheten

Title: Methods for localizing and quantifying radionuclide sources and deposition using in situ gamma spectrometry

Abstract

This thesis describes investigations made on mobile and stationary gamma spectrometry made both under laboratory conditions and *in situ.* The objective has been to identify and quantify radionuclides in the form of point sources, contamination and widespread deposition in situations where the measurement geometry is not known beforehand. Both scintillators and semiconductor detectors of similar size were tested in a backpack configuration in the vicinity of an unmapped underground waste storage in the Republic of Georgia. The results showed that a high efficiency HPGe detector (>100% relative efficiency) was the best choice with respect to sensitivity compared to $LaBr_3$(Ce) and NaI(Tl) detectors. It was also the most cumbersome system of them all in terms of field operability due to the liquid nitrogen. The evaluation method of plotting the full energy peak count rate on maps worked well, especially when assessment of the maps was made offline by an external base support, which speeded up the field work significantly. A large part of the thesis has been focused on evaluating and using the so-called peak-to-valley method (PTV method). Measurements and simulations to investigate components in the pulse height distribution contributing to the PTV ratio have been done both in a laboratory and outdoors in a controlled radiation environment as well as *in situ*. The PTV studies have been focused on investigating how well the method works for quantification of ^{137}Cs, with the aim of either finding a reliable point source depth, or a factor to correct the estimated surface equivalent mean deposition *in situ,* compensating for the shielding effects brought on by the ground penetration of ^{137}Cs. In order to better understand the scatter processes of ^{137}Cs photons in the air, ground, and the surrounding material of the detector, simulations in MCNP5 and measurements have been performed in various configurations. The simulations and measurements performed with a well-characterized HPGe detector in a low gamma background room, revealed a 25% difference in full energy peak efficiency between simulation and measurement for 662 keV photons from ^{137}Cs. The inner components of a detector appeared to have significant impact on agreement between simulation and measurement and components contributing to this impact were identified. Regarding the PTV ratio three HPGe detectors were compared with respect to their angular PTV ratio response, to prepare for a sensitive approach on estimating deposition penetration depth of ^{137}Cs *in situ.* Detectors of sizes ranging from 18% to 123% in relative efficiency showed similar PTV ratios for incident angles between 0° and 90° when using a 30 keV valley interval. The point source measurements showed that a field of view of about 3 m in radius was a good choice presenting the possibility to resolve whether the deposition is on the ground surface or has penetrated beneath the surface. When the detector systems were brought to the fallout areas outside Fukushima Daiichi in Japan, the evaluation of the PTV ratios showed perturbation, which was ascribed the presence of ^{134}Cs. The laboratory investigations of this perturbation showed a significant disturbance down to a ^{134}Cs:^{137}Cs ratio in the deposition of 1:100. To follow up on earlier results indicating an improvement in the reliability of the PTV ratio for both ^{137}Cs and ^{134}Cs, a collimator was applied at the *in situ* measurement locations in the Fukushima Daiichi region. The collimation increased the PTV ratio significantly for ^{134}Cs but not so for ^{137}Cs when both radionuclides were present. This indicated that the ^{134}Cs PTV ratio should be used instead of that for ^{137}Cs the first decade after an accident where both cesium radionuclides are released. If no ^{134}Cs is present the collimator will successfully improve the ^{137}Cs PTV ratio due to the advantages of limiting incident angles to those close to the detector.

Key words		
Classification system and/or index terms (if any)		
Supplementary bibliographical information		Language: English
ISSN and key title		ISBN: 978-91-7753-240-8
Recipient's notes	Number of pages:	Price
	Security classification	

Signature  Date 2017-04-28

Methods for localizing and quantifying radionuclide sources and deposition using *in situ* gamma spectrometry

Critical review of the peak-to-valley method based on experimental studies and applications in Georgia and Japan

Karl Östlund

LUND
UNIVERSITY

Medical Radiation Physics
Department of Translational Medicine, Malmö
Faculty of Science, Lund University
2017

Cover photo by Patrick Kenny, IAEA,
“measurements in Fukushima in the afternoon”
Copyright Karl Östlund
Doctoral Dissertation
Lund University
Faculty of Science Doctoral Dissertation Series
Medical Radiation Physics, Malmö
Department of Translational Medicine, Lund university
Skåne University Hospital
SE-205 02 Malmö, Sweden
ISBN 978-91-7753-240-8
Printed in Sweden by Media-Tryck, Lund University
Lund 2017

To my family,
and to the memory of one of my best friends, Karin Lindh, I miss you.

Content

Abstract

This thesis describes investigations made on mobile and stationary gamma spectrometry made both under laboratory conditions and *in situ.* The objective has been to identify and quantify radionuclides in the form of point sources, contamination and widespread deposition in situations where the measurement geometry is not known beforehand. Both scintillators and semiconductor detectors of similar size were tested in a backpack configuration in the vicinity of an unmapped underground waste storage in the Republic of Georgia. The results showed that a high efficiency HPGe detector (>100% relative efficiency) was the best choice with respect to sensitivity compared to $LaBr_3$(Ce) and NaI(Tl) detectors. It was also the most cumbersome system of them all in terms of field operability due to the liquid nitrogen. The evaluation method of plotting the full energy peak count rate on maps worked well, especially when assessment of the maps was made offline by an external base support, which speeded up the field work significantly. A large part of the thesis has been focused on evaluating and using the so-called peak-to-valley method (PTV method). Measurements and simulations to investigate components in the pulse height distribution contributing to the PTV ratio have been done both in a laboratory and outdoors in a controlled radiation environment as well as *in situ*. The PTV studies have been focused on investigating how well the method works for quantification of ^{137}Cs, with the aim of either finding a reliable point source depth, or a factor to correct the estimated surface equivalent mean deposition *in situ,* compensating for the shielding effects brought on by the ground penetration of ^{137}Cs. In order to better understand the scatter processes of ^{137}Cs photons in the air, ground and the surrounding material of the detector, simulations in MCNP5 and measurements have been performed in various configurations.

The simulations and measurements performed with a well-characterized HPGe detector in a low gamma background room, revealed a 25% difference in full energy peak efficiency between simulation and measurement for 662 keV photons from ^{137}Cs. The inner components of a detector appeared to have significant impact on agreement between simulation and measurement and components contributing to this impact were identified.

Regarding the PTV ratio three HPGe detectors were compared with respect to their angular PTV ratio response, to prepare for a sensitive approach on estimating deposition penetration depth of ^{137}Cs *in situ.* Detectors of sizes ranging from 18% to 123% in relative efficiency showed similar PTV ratios for incident angles between 0° and 90° when using a 30 keV valley interval. The point source measurements showed that a field of view of about 3 m in radius was a good choice presenting the possibility to resolve whether the deposition is on the ground surface or has penetrated beneath the surface.

When the detector systems were brought to the fallout areas outside Fukushima Daiichi in Japan the evaluation of the ^{137}Cs PTV ratios showed perturbation, which was ascribed the presence of ^{134}Cs. The laboratory investigations of this perturbation showed a significant disturbance down to a ^{134}Cs:^{137}Cs ratio in the deposition of 1:100. To follow up on earlier results indicating an improvement in the reliability of the PTV ratio for both ^{137}Cs and ^{134}Cs, a collimator was applied at the *in situ* measurement locations in the Fukushima Daiichi region. The collimation increased the PTV ratio significantly for ^{134}Cs but not so for ^{137}Cs when both radionuclides were present. This indicated that the ^{134}Cs PTV ratio should be used instead of that for ^{137}Cs the first decade after an accident where both cesium radionuclides are released. If no ^{134}Cs is present the collimator will successfully improve the ^{137}Cs PTV ratio due to the advantages of limiting incident angles to those close to the detector.

Summary in Swedish
(Populärvetenskaplig sammanfattning)

Inom beredskapen mot radiologiska och nukleära olyckor och katastrofer spelar strålningsmätningar en avgörande roll för att ta redan på vad som har hänt och hur farligt det är för människa, djur och natur och på vilket sätt det påverkar samhällsfunktioner. Allmänheten har rätt att få reda på vad som hänt och vilka konsekvenserna kan tänkas bli. För detta behövs strålningsmätningar som utförs direkt efter olyckan samt under en lång period därefter. Olyckorna eller händelserna kan vara begränsade i utbredning eller påverka gigantiska landområden. Den gemensamma faktorn kring dessa händelser och platser är att man vet väldigt lite i början om vad som hänt eller hur läget egentligen är. Mätningar i olika skeden behövs löpande, för att myndigheter skall kunna göra korrekta bedömningar och ta rätt beslut.

Mätningarna direkt efter olyckan eller händelsen syftar till att ta reda på var de radioaktiva ämnena tagit vägen och hur mycket som finns på eller i marken. Ofta räcker det med att mäta doshastigheten och att ta reda på vilka radioaktiva ämnen som kommit ut. Snart uppstår högre krav på mätningarna och detaljnivån som efterfrågas är högre.

För att kunna göra uppskattningar av hur stråldosen till invånarna i olika delar av samhället kommer utveckla sig, behöver man i ett senare skede veta mer om hur de radioaktiva ämnen som släppts ut förflyttar sig i miljön, både mellan olika platser och hur de tränger ner i marken. Om ett ämne relativt snabbt sjunker ned i marken så minskas stråldosen till människan ganska mycket bara för några centimeters nedträngning. Detsamma gäller när marken täcks av snö. Sådan information är viktig när det gäller att göra prioriteringar i arbetet att sanera efter olyckan. Det blir samtidigt viktigare och viktigare för myndigheter att kunna stödja sig på fakta för att vinna allmänhetens förtroende när åtgärder gör intrång i enskildas människors liv som upplevs svåra att acceptera.

De radioaktiva ämnen som har visat sig vara av störst betydelse vid de två senaste kärnkraftsolyckorna är ^{134}Cs och ^{137}Cs (cesium). Avhandlingen har försökt att förbättra en befintlig metod som kallas peak-to-valley metoden, för uppskattningar var i marken radioaktiviteten befinner sig. Metoden utnyttjar olika delar av en detektors pulshöjdsfördelning för att ge mer information än bara mängden radioaktiva ämnen på marken. Metoden är till för att försöka visa var det radioaktiva cesiet befinner sig i marken.

Avhandlingen har utforskat nya sätt att applicera metoden. Genom att använda en tjock blycylinder runt detektorn som hindrar strålning från längre avstånd att nå detektorn, kan man på ett noggrannare sätt ta reda på nedträngningsdjupet. Samtidigt

får man reda på hur mycket radioaktivitet som finns på marken, fast för en betydligt mindre yta. Det finns en rad andra intressanta applikationer för en sådan metod, vilka kan vara väldigt intressanta att utforska i framtiden.

Original papers

This thesis is based on the following papers, which will be referred to in the text by their Roman numerals.

I. **Tests of HPGe- and scintillation-based backpack γ-radiation survey systems.** Nilsson, J., **Östlund, K.**, Söderberg, J., Mattsson, S., Rääf, CL. Environ Radioactiv 135, 54-62, (2014).

II. **Experimentally determined vs. Monte Carlo simulated peak-to-valley ratios for a well characterized n-type HPGe detector. Östlund, K.**, Samuelsson, C., Rääf, C.L. Appl Radiat Isotopes, 95, 94–100, (2015).

III. **Peak-to-valley ratios for three different HPGe detectors for the assessment of ^{137}Cs deposition on the ground and the impact of the detector field-of-view. Östlund, K.**, Samuelsson, C., Mattsson, S., Rääf, C.L. Appl Radiat Isotopes, 120, 89-94, (2017).

IV. **The influence of ^{134}Cs on the ^{137}Cs gamma-spectrometric peak-to-valley ratio and optimization of the peak-to-valley method by limiting the field of view. Östlund, K.,** Samuelsson, C., Mattsson, S., Rääf, C. L. Appl Radiat Isotopes (revision requested and submitted) (2017).

Abbreviations

ARS	Acute Radiation Sickness
CT	Computed Tomography
EBS	External Base Support
Γ-constant	A radionuclide specific dose-rate value per unit activity
HASS	High Activity Sealed Source
In situ spectrometric measurements	Measurements made (in this work) under field circumstances or outdoors. *In situ* is a Latin phrase that translates literally to "on site"
keV	Radiation energy unit
LBC	Low Background Counting
MCNP5	Monte Carlo N Particle code version 5
MCNPX	Monte Carlo N Particle code for simulation of heave patricles and ions
PTC	Peak-to-Compton ratio, a quality factor for detectors.
PTV	Peak-to-valley
rel. efficiency	Detection efficiency of a detector relative to a 76.2 mm (Ø) by 76.2 mm NaI(Tl) detector at 1332 keV and a distance of 25 cm.
ROI	Region of Interest
RTG	Radio Thermal Generator
SDI	Spectrum Dose Index, a dose-rate calculated by multiplying the number of detected pulses in a pulse height distribution by an energy dependent factor to present the total photon dose-rate.

1 Introduction and objectives

1.1 Background

Both local and more widespread dispersion can occur with radioactive substances. Dispersion could be accidental or deliberate, but the presumed risk has to be estimated regardless of reason. This estimation could be made in an early stage by simplified prognosis and predictions of the extent of the radiological impact, more detailed information is eventually needed about radiation levels and the magnitude of the source strength that is out of control. The source strength can be estimated in terms of, for example, total activity, activity concentration, or surface deposition. If it is a point source and the radionuclide has been identified, the most common estimation method is use of the "Γ-constant", which relates the absorbed dose rate in air at a reference distance (typically 1 m) from the point source to the activity of the source. When the source is dispersed in a larger area (e.g., ≥100 m^2), one can still use a specific Γ-constant, but a gamma spectrometer is needed for more detailed measurements.

The spectrometer has to be calibrated for measuring area sources *in situ*. This calibration can be performed several ways in the laboratory using point sources, mathematical simulation software such as Monte Carlo codes, or commercial software based on analytical calculations (ISOCS®, ISOTOPIC®). In the laboratory, calibration is usually performed by measuring the photo peak efficiency at the incident angles and a determined distance, usually 1 m and between 0° and 90° with a 10° angle increment (Beck et al., 1972, Finck, 1992). The photo peak efficiency of the detector for each angle is then multiplied by the peak count rate per second, corrected for air attenuation and distance, and then integrated between 0° and 90°. This is still the most commonly used method, but it is labor intensive and sensitive to the accuracy of the geometrical setup. The use of Monte Carlo codes simplifies the investigation of the angular efficiency of a detector, but describing the detector geometry in the input file usually takes a substantial amount of time. Available commercial software is often expensive and needs to be validated against calibrated sources. Thus, the computer or semi-computer based methods require a user with sufficient knowledge of how to correctly build the input geometries in order to achieve acceptable accuracy.

An accident involving reactor failure presents the possibility of releasing a substantial amount and wide range of radionuclides. The release of radionuclides is dependent on the core temperature of the reactor and the release pathways out of the broken reactor vessel. Looking back at the two major releases at Chernobyl and Fukushima Daiichi, over time there have been only a few important radionuclides in terms of external exposure to the public, basically due to their long physical half-life and significant Γ-constant. In this respect, the two cesium isotopes ^{134}Cs and ^{137}Cs are often referred to as the most relevant isotopes in terms of external radiation dose impact ^{134}Cs has a high Γ-constant but due to its physical decay is negligible after 15-20 years. While ^{137}Cs continues to contribute to the radiation dose up to at least 80-100 years. However, one cannot discard the radionuclides with shorter half-life that contribute to the external radiation dose at the beginning of the accident, such as ^{131}I, ^{132}I, ^{103}Ru/^{103}Rh, ^{106}Ru/^{106}Rh, and ^{90}Sr.

1.2 The peak-to-valley method

The idea of the peak-to-valley (PTV) method is based on full energy photons from, for example, ^{137}Cs scattering with a small loss of energy (i.e., a small Compton scatter angle). When these photons are detected by an *in situ* spectrometer, they end up in an energy region just below the full energy peak in the pulse height distribution (Figure 1). The PTV ratio was introduced in 1992 by Peter Zombori, who aimed to correlate the ^{137}Cs full energy peak net counts and the net counts in a 20 keV valley just underneath the full energy peak to a depth distribution (Zombori et al. 1992, Zombori et al., 1992b).

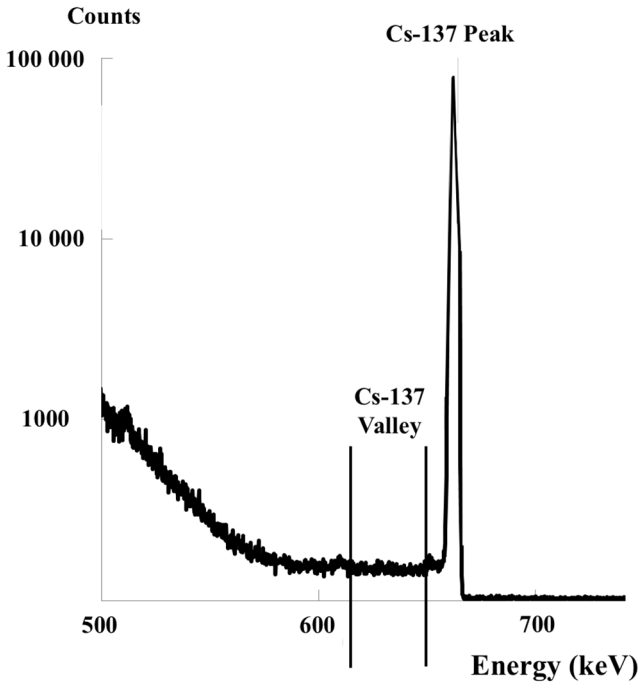

Figure 1.
A representative pulse height distribution with the peak and valley region, measured in the LBC room.

The equation for the PTV ratio can be written as Eq. 1:

$$PTV(E) = \frac{P(E)}{V(\Delta E')} \qquad \text{Eq. 1}$$

Where $P(E)$ is the net peak counts of the peak with energy E and $V(\Delta E')$ is the net valley counts in a chosen valley region with width $\Delta E'$.

In Paper II the ratio was expressed in a similar manner (Eq. 2) in order to take into account the electronic settings and resolution of the full energy peak. E_γ is the peak energy, ROI_{peak} is the net number of counts in the full energy peak, ROI_{Valley} is the net number of counts in the chosen valley region of interest (ROI) below the full energy peak, n is the lower energy limit, and a *is* the width of the chosen valley ROI. FWHM in Eq. 2 is the full width at half maximum obtained in the pulse height distribution, incorporating the settings of the electronics and intensity of the photon radiation field. k is a detector-specific variable, used to relate an adapted ROI, ROI_{peak} to the photo peak in the pulse height distribution. A typical value for k for HPGe detectors is close to 1.5.

$$PTV = \frac{ROI_{Peak}[E_\gamma - k \cdot FWHM, E_\gamma + k \cdot FWHM]}{ROI_{Valley}[n,(n+a)]keV} \quad \text{Eq. 2}$$

When choosing the ROI_{Valley} range and position beneath the full energy peak, the user also chooses the allowed scatter angles for the primary photons, in order to register in the valley. Equation 3 estimates the minimum and maximum allowed scatter angle:

$$h\nu' = h\nu \frac{1}{1+\alpha(1-cos\theta)}, \quad where \quad \alpha = \frac{h\nu}{m_0 c^2} \quad \text{(Eq. 3)}$$

Where $h\nu$ is the initial primary photon energy, $h\nu'$ is the energy of the Compton scattered photon, θ is the photon scatter angle, and $m_0 c^2$ is the resting mass of the electron expressed in energy (511 keV). Typical scatter angles for a suitable position of the valley underneath the full energy peak of ^{137}Cs are approximately 9° to 20°, where 20° is the maximum scatter angle (i.e., the scattered photon energy *n* in Eq. 2.) The gross number of counts in the valley ROI has several different origins (Figure 2). The detector itself contributes to counts in the valley due to single and multiple scatter interactions in the surrounding detector components or inside the detector itself. This component of the total gross count is estimated by measuring the PTV ratio in an environment without background and with a scatterless source (Figure 2, LBC). The natural background normally contributes a higher count rate to the valley than the scattered photons induced by the detector. This component is estimated by measuring the contribution to the PTV ratio *in situ* at a representative location without fallout (Figure 2, Bkg). Both contributing factors have to be subtracted from the PTV ratio measured *in situ* with fallout on the ground (Figure 2, Japan). A background valley is usually used on the right side of the full energy peak to compensate for background *in situ* (Gering et al., 1998). When viewing the natural background counts in this background valley ROI, the ratio between the valley ROI on the left and the background valley ROI on the right side of the peak, will likely not change significantly between locations.

The PTV ratio is not dependent on photon peak yield other than needing to generate enough counts in the valley to increase significantly above the background. However, the ratio is dependent on the photon cross section of the ground material. The total cross section of the ground material is dependent on both the elemental composition of the soil in the ground, including its water content, and on the energy of the emitted full energy photons. This, in turn, requires that the energy of the full energy peak is suitable for the material in the ground (i.e., that the cross section of photons and density of the ground material is sufficient to produce enough scattered photons). To avoid interference in the background counts, peaks of higher energy (>1200 keV) are preferred. However, the attenuation and scatter cross section of these energies in

normal soil are low, resulting in poor valley counting statistics. When choosing a peak energy in the 50 – 200 keV range, the loss of peak counts due to attenuation in the ground is higher. In combination with a relatively higher background count rate from Compton scattered photons originating from higher energies, the combination is unfavorable for PTV ratio quality. Zombori et al. in 1992 related the PTV ratio to a vertical depth distribution of ^{137}Cs deposition in the ground. They found a correlation between the PTV ratio and the distribution model described by a double exponential function (Lorentz function, Eq. 6) for fallout from Chernobyl in Belarus a couple of years after the nuclear power plant accident.

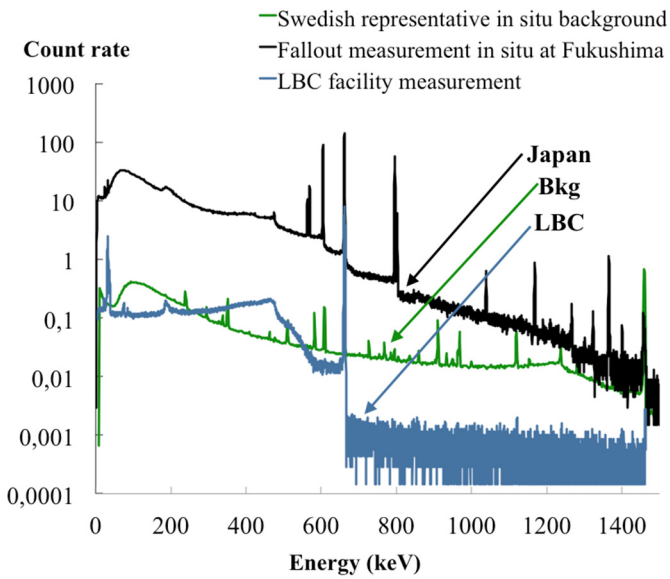

Figure 2.
Three pulse height distributions, a low background counting (LBC) room reference pulse height distribution (^{137}Cs), a background reference pulse height distribution acquired *in situ* (Bkg), and the result of a typical measurement outside Fukushima Daiichi. The count rate per second in each channel is plotted and the parameters that contribute to the PTV ratio are visible, i.e., the internal detector contribution (LBC), a contribution from the natural background (bkg), and the pulse height distribution appearance when measuring fallout years after the release in Fukushima (Japan).

The accuracy of the PTV ratio increases with control of factors, such as the flatness of the ground, counting statistics, the homogeneity of the source, and whether the source is on the ground surface or further down in the ground.

Before the study by Zombori et al. in 1992, others had shown an interest in extracting more information from the pulse-height distributions measured *in situ* than just the net counts in the full energy peak. Karlberg investigated different approaches to compensate for the decrease in the uncollided flux of primarily ^{137}Cs due to ground

penetration in order to more accurately estimate the deposition (Bq/m^2) (Karlberg, 1990).

Several others have presented investigations after the introduction of the PTV method in 1992 and used it as a tool to estimate ground distribution assuming a predefined depth distribution model (Baeza and Corbacho, 2010, Fulöp and Ragan 1997, Gering et al. 1998, Hjerpe and Samuelsson, 2002, Kastlander et al., 2005, Lemercier, 2008, Panza, 2012, Tyler et al., 1996, Tyler, 1999, Tyler, 2004).

Tyler et al., Gering et al., Fulöp and Ragan, Hjerpe and Samuelsson, have used the PTV method with modifications in order to explore its possibilities, with different valley range and methods to estimate background. Gering et al. made a successful attempt to estimate the background by simulations and then compensating measured PTV values by subtracting the estimated background. Kock and Samuelsson in part investigated how the parts of the detector contribute to the PTV ratio by computer modeling in MCNP5 (Kock, 2007). Efficient computer modeling of the detector and irradiation setup as we experience it today was not possible until approximately 10 years ago. When sufficiently powerful computers became available as personal computers, the possibilities opened up for further studies of the PTV ratio and its strengths and weaknesses.

In retrospect, Gering et al. in 1998 presented an uncertainty estimation based on the counting statistics, which presented relative uncertainty of approximately 2 to 8% for a 30 keV valley ROI and a variety of ground types. Gering et al. also discussed the variation in the contribution from natural radionuclides and cosmic radiation. This is important in situations in which low levels of contamination are measured but generally negligible in the context of ^{137}Cs levels above 50 kBq/m^2.

1.3 Sources and depth distribution models

A number of models could be used to describe the depth distribution of relatively fresh fallout (up to or a few years old). One model introduced by Lidström et al. in 1998 assumes a single slab model in which the deposition is confined in the top layer (i.e., slab of standard soil with a thickness of approximately 1-2 cm, $\rho=0.5 g/cm^3$). This model further assumes that the deposition is uniformly distributed within the slab and the surface roughness can be successfully accounted for by adjusting the slab density (Lidström et al., 1998). A two-slab model could also be used if the fallout has penetrated the surface (ICRU Report 53, 1994, Thummerer and Jacob 1998).

Applying the exponential relaxation model, which is widely considered to be a good enough approximation of the true distribution of more than 1-year-old fallout, the

deposition is expected in the topsoil layer and partially penetrating into the ground (Finck, 1992). The exponential distribution can be described by the Eq. 4:

$$c(z) = c_0 \cdot e^{-\frac{\alpha}{\rho}\rho \cdot z} \qquad \text{Eq. 4}$$

Where c_0 is the radioactivity concentration at the surface of the ground, $\frac{\alpha}{\rho}$ is the exponential mass activity distribution coefficient, ρ is the soil density, and z is the depth (Isaksson and Rääf, 2016).

After approximately a decade, the radionuclide distribution has gradually changed and the deposition is often considered to have left the soil surface. This migration downward is due to several processes in which a number of ecological processes interact. The soil surface obtains new biological material from leaves and green matter, and a relatively clean layer builds up on top of the contaminated surface. Rain, agriculture, and human activities transport the radionuclides downward into the ground (Yoschenko, et al., 2006; Lemercier, 2008; Panza, 2012). A decade after the release, the ^{134,137}Cs could be distributed with a maximum radionuclide concentration further in the ground and would be better described by a Lorentz function as in Eq. 5.

$$A_m(\zeta) = \frac{A_1}{(\zeta - A_2) + A_3^2} \qquad \text{Eq. 5}$$

Where $A_m(\zeta)$ is the activity per unit mass (Bq/kg), and ζ is the soil mass per unit area (g/cm^2) (see Eq. 6). A_1 is a scaling factor to reach the correct magnitude of the activity concentration, and A_2 and A_3 are parameters that describe the location of the radioactivity and the width of the maximum concentration of radioactivity (Hillman et al., 1996; Hjerpe et al., 2002).

The mass depth, ζ (g/cm^2) can be expressed as:

$$\zeta = \int_0^z \rho(z')\, dz' \qquad \text{Eq. 6}$$

Where $\rho(z')$ is the material density (g/cm^3) as a function of depth.

1.4 Measurement situations presenting challenges for equipment and operators

1.4.1 Lost or dispersed sources

Radioactive sources with high activity (i.e., high activity sealed sources [HASS] and similar sources) have historically been lost. In one incident in Goiania in 1987, the source capsule of a stolen ^{137}Cs source was unfortunately opened and the source dispersed over a large area of several city blocks (IAEA, 1988). Another example is the re-entering of the Russian COSMOS 954 satellite in 1978 into Earth's atmosphere while carrying a ^{235}U reactor to supply the unit with electrical power. The reactor core broke up in the atmosphere upon re-entry and was scattered over a large area in Canada (Heaps, 1978).

Old repositories originating from 30-50 years ago are still present in various parts of the world. These storage sites are not all well documented, well guarded, or well protected. The radiation protection authorities in these countries, and in other cases, owners of radiation sources in the world have not properly handled or stored radiological or nuclear material for a long period of time. Their capacity to investigate the situation today is often limited. Current views on the environment, awareness, and internationally accepted guidelines necessitate actions that bring these sources under control. The variety of possible scenarios in these situations is expected to be wide ranging, from deeply buried point sources to well-shielded sources. Another situation could be a source predominantly producing sky-shine. As there is often very little information to begin with, there is a need for able personnel and instruments.

1.4.2 Accidents and deliberate actions involving fissile material

The radionuclide inventory in an operating reactor core differs from the inventory resulting from a detonation of a nuclear weapon. This is due to the fact that a nuclear reactor has operated for a period of time, which builds up the inventory of long-lived radionuclides. As an example the amount of ^{134}Cs is expected to be a 1000 times less or even a smaller amount compared to the amount of ^{137}Cs, after a nuclear weapon detonation compared to a reactor accident. Hence, it is a completely different measurement situation, as dose-rates after a nearby nuclear weapon detonation initially would be several orders of magnitudes higher, since it is released instantly to the environment, and measurements then have to aim primarily at aiding the survival of the inhabitants. The measurements after the failure of a nuclear reactor, on the other hand, since its expected to be a slower process releasing less short-lived

radionuclides, will mainly aim at protection, the survival of the community, economy, and way of life in affected areas. The radionuclides in the fallout from a nuclear detonation are determined by, for example, the yield and type of nuclear weapon, if the explosion was close to the ground. The deposition consists of all short-lived radionuclides, and would severely affect the targeted and surrounding countries. When addressing the reactor failure, the number of radionuclides present at the site of investigation *in situ* may be approximately 100 or more depending on the time after deposition. For a nuclear power plant, the fuel temperature, radionuclide inventory of the reactor, and characteristics of the reactor failure would determine the content of the released radioactivity. Many of the radionuclides that have a short half-life, including ^{132}I and ^{136}Cs, and will disappear quickly with marginal radiological impact, but other radionuclides with longer half-lives (i.e., ^{134}Cs, ^{137}Cs, and ^{90}Sr) remain in the environment for a long period of time.

In the case of a reactor failure, different radionuclides will become mobile at different temperatures (boiling points) and, if not contained, will be released into the atmosphere and end up on the ground by dry or wet deposition. The radionuclides are often described from the viewpoint of how volatile they are, as the radionuclides that become mobile at fairly low temperatures are the most volatile. A temperature-graded table is presented in Figure 3 as an example of what was released at Three Mile Island, Fukushima Daiichi, and Chernobyl.

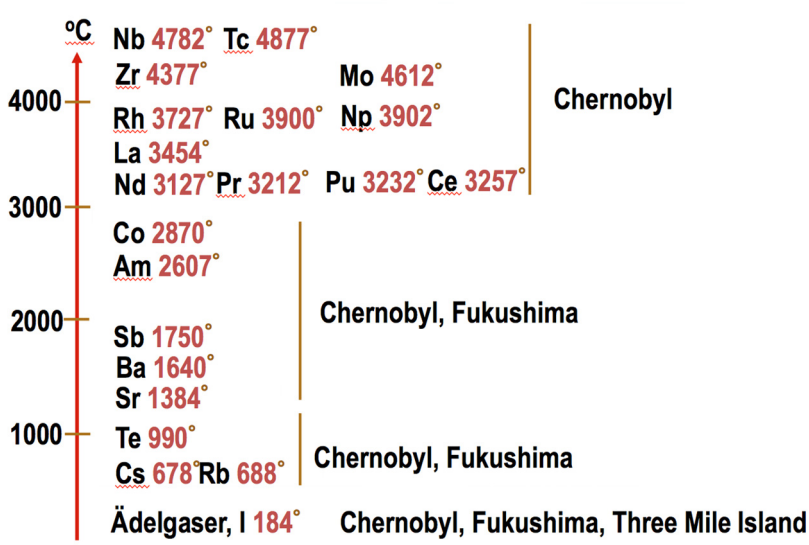

Figure 3.
Common radionuclides and their boiling points in combination with their abundance in three major reactor accidents. In the Fukushima accident, ^{129m}Te, ^{89,90}Sr, and very low levels of ^{238,239,240}Pu isotopes have been observed *in situ* and the estimated reactor core temperature was set to a maximum of 2100-2300°C (Yoshida and Takahashi, 2012). (The original figure was obtained from the Swedish Radiation Safety Authority´s educational material and has been edited by the author).

The severity of a reactor failure depends on many factors. The management of the accident is dependent on human actions, which could mitigate or aggravate the development and consequences to the environment. If one would attempt to grade the severity of the three major accidents that have occurred thus far, Chernobyl was the worst accident by several orders of magnitude (UNSCEAR, 1988, 2000, 2013; Buzulukov and Dobrynin, 1993). The Chernobyl reactor failure occurred during operation of the reactor, and the core was exposed to free air for several months afterwards, presenting a very difficult situation from a measurement perspective. This is the only reactor accident in its initial phase to cause several deaths due to radiation exposure causing acute radiation syndrome (ARS), and could potentially have caused a severe situation in the village of Pripyat, if the heat in the released plume or the weather had been different (Buzulukov and Dobrynin, 1993, Mosey, 1990). Chernobyl released a large number of radionuclides into the environment and serves as an example of the upper end point in operator difficulty for *in situ* measurements.

The aforementioned situations with unknown prerequisites in terms of source types or positions place further demands on the methods for searching and mapping and on the detector systems. The use of the scattered component in the pulse height distribution during *in situ* measurements, from both backpacks and stationary equipment, can help the operator come to a more accurate decision regarding ground penetration and the total activity per unit area of the source.

1.5 Purpose of *in situ* gamma spectrometry

There are several reasons for the measurements that are to be performed if a nuclear accident occurs. One example of a country where this may occur is Sweden, as it has several domestic nuclear power stations. There are strategic reasons why emergency preparedness is needed and funded in Sweden. Sweden is a democracy with a legal system providing society with insight into governmental actions and decisions. The emergency preparedness measurements are built on three major points (Radiakskyddsberedskap 2000, 1998; FOA C40324, 1994, Nisbet, 2010, Nisbet, 2015a, Nisbet 2015b). Measurements in the emergency organization are needed for protection, information, and documentation.

1.5.1 Protection

Initial fast actions on protection will be made on preplanned decisions, such as evacuation and staying indoors. To protect the public the authorities need facts about the accident to perform their tasks, which is to protect the community.

Measurements are needed to make correct decisions in the time following the initial fast actions.

I general and practical terms one realizes that after a nuclear accident or nuclear bomb detonation the important issue is the protection of the public health. Initial measurements that are performed are predominantly measurements of the external dose-rate in the affected areas if possible. This is done with either mobile system, stationary dose-rate instrumentation in an array over the region, or by measurements in pre-defined strategically chosen positions in the affected area. *In situ* measurements are performed during the initial phase to provide a first insight to the situation.

1.5.2 Information.

Information about the situation is needed in order to successfully perform the rescue work necessary to protect people, property, and the environment in an emergency situation. In addition, the public has the right to know what is happening. The public should be informed, and the core issue is that everybody should understand the situation. In order to present the situation properly in different phases in an accident or malevolent act, the authorities need spectrometric information as a basis for this communication to the public.

There is a clear psychological need for the public to receive information, to understand the extent of the accident, and to better manage their day-to-day life in the context of the new situation.

1.5.3 Documentation

This part of the strategy provides the investigation with the details of what went wrong, why it happened, and to what society was exposed. This part could resemble a historical overview of the accident and will present the reasons why the new situation in the community turned out the way it did.

The radioactivity released into the environment by either a nuclear weapon detonation or a reactor accident could include a number of radionuclides. Through *in situ* measurements, it is possible to determine which radionuclides were released (Edvardsson, 1991; Finck, 1992). The different radionuclides have different half-lives and different ways of contributing to the radiation dose to the individual, as the radionuclides emit different types of radiation (α, β, and γ). The contribution to the radiation dose by released radionuclides is also very different with respect to internal and external exposure.

1.5.4 *In situ* measurement challenges

There are additional challenges when using instrumentation designed for "normal" background situations, during an emergency situation with perhaps much higher radiation levels. After some time, additional information about the radionuclide content of the fallout and deposition in the ground is needed to calculate the time-dependent development of the public accumulated dose. As previously mentioned the deposited radionuclides have different physical half-lives and, by determining the radionuclide composition, the decrease in dose rate over time can be predicted. The radionuclide composition also provides information on the reactor status in different stages of the accident, such as the temperature inside the reactor core. This information was difficult to obtain for the accident in Fukushima Daiichi (Japan) due to the damage caused to the nuclear power plants by the earthquake and tsunami.

However, there are a number of challenges in producing measurement results with good enough quality in accident situations, which will be valid for a long period of time. For example, the total count rate in the pulse height distribution when measuring *in situ* may be well beyond recommendations for the instrument. Unfortunately, this can generate dead times in the *in situ* measurement systems ranging from as an example 20% to close to 100%. The high photon flux rate may cause summation between photons of identical energy and between photons of different energies. As a practical example, within the work done in this thesis, slightly distorted full energy peaks double and triple the primary ^{137}Cs photon energy were observed when conducting measurements in Japan in areas with substantial fallout. This creates a pulse height distribution background for the operator performing *in situ* measurements that is very different from normal operations. Given all these factors the operator needs optimized equipment and accurate training to present accurate results that can serve the *protection, information,* and *documentation* demands of the accident.

1.6 Objectives

The overall objective of this PhD thesis was to further investigate the possibilities of localizing and quantifying both radioactive point and dispersed sources using *in situ* measurements. Four studies were conducted to meet this objective. They were carried out in the laboratory as well as *in situ* in Sweden, Georgia (Caucasus, Eurasia region), and Fukushima (Japan). The specific aims of each study are presented below:

I. The first objective in Paper I was to investigate whether large HPGe and $LaBr_3(Ce)$ detectors contributes with added value in backpack configurations for locating point or volume sources in areas up to 10^5 m^2 compared to traditional portable detectors of NaI(Tl).

II. In Paper II, the PTV ratio for ^{137}Cs primary photons (662 keV) for a well-characterized gamma spectrometer was investigated using both measurements and Monte Carlo simulations to determine how the detector characteristics affect the PTV ratio. This was done by evaluating the agreement between simulations and measurements under optimized laboratory conditions and by varying different detector parameters.

III. In Paper III, the differences in the PTV ratio for different incident angles of ^{137}Cs were investigated for three different n- or p-type HPGe detectors. In addition, an attempt was made to investigate how the PTV ratio depends on the distance between the detector and a point source at the surface or submerged 1 and 2 cm in the ground.

IV. In Paper IV, the disturbance from ^{134}Cs when determining the ^{137}Cs PTV ratio was investigated. Whether the ^{134}Cs PTV ratio could be used instead of the ^{137}Cs ratio was also investigated. In addition, the paper examined the possibility of improving the PTV ratio by using collimators.

2. Material and methods

2.1 Detectors

2.1.1 Scintillation detectors

In Paper I, a 76.2 mm (Ø) by 76.2 mm $LaBr_3$(Ce)scintillation detector and an 84.0 (Ø) mm by 85.8 mm (123% rel. efficiency) HPGe detector were used for all measurements (see Table 1). Gammadata Instruments in Uppsala (Sweden) assembled the $LaBr_3$(Ce) detector in an aluminum tube with 1 cm voluminous polyurethane pads acting as thermal insulation between the tube and the detector. This detector is very suitable for fieldwork, including travel because it does not require cooling and can be started within minutes after arrival. A drawback of this detector is that it contains ^{138}La and ^{227}Ac, creating disturbances in the background of the measurements in the form of a primary photon peak at 1436 keV, and peaks from internal α and β radiation (Milbrath et al., 2005). However, if the full energy peak of the radionuclide in question is located in a region with a lower background count or is intense enough to render the internal and natural background insignificant, then the detector is useful for most *in situ* gamma spectrometric applications. The material in this detector also yields a better full energy peak efficiency than the standard NaI(Tl) scintillation detector or HPGe detector, and the usability in high-intensity radiation fields are also better than the others due to the short afterglow in the detector material. When quantifying low activity levels or searching for sources with an unknown location, larger detectors with their higher counting efficiencies are preferred. The NaI(Tl) detector is the most widely used and superior in terms of cost and efficiency. Hence, large NaI(Tl) detectors are used in search applications as either single detectors or arrays.

Table 1.
An overview of the detectors used in this thesis. Relative efficiency refers to the full energy peak effeiciency of a 76.2 mm (Ø) by 76.2 mm NaI(Tl) detector at 1332.5 keV at a distance of 25 cm.

Detector type	Window/Assembly	Detector dimensions	FWHM (662 keV)	Relative efficiency
n-type	Be (0.5 mm)/Al (1.5 mm)	45.1 mm(diam.) x 73.8 mm	1.6 keV	18.0%
p-type	Al (1.0 mm)/Al (2.6 mm)	57.8 mm(diam.) x 42.5 mm	1.3 keV	26.1%
p-type	Al (1.5 mm)/Al (3.0 mm)	84.0 mm(diam.) x 85.8 mm	1.7 keV	123.0%
NaI(Tl)	Al (2.0 mm)/Al (2.0 mm)	76.2 mm (Ø) by 76.2 mm	40 keV	100%
$LaBr_3$:Ce	Al (2.0 mm)/Al (2.0 mm)	76.2 mm (Ø) by 76.2 mm	25 keV	130%

2.1.2 Semiconductor detectors

The HPGe detector has superior energy resolution compared to all other detectors used in this thesis for fallout and field applications. In situations in which a large number of full energy peaks are present and the input count rate is within the limits of the detector system, this detector type is often the only option. For field applications, the coaxial detector is usually chosen for its uniformity in angular efficiency between 0° and 90° compared to e.g. planar detectors. The background pulse distribution is dependent on the detector size. Small detectors with approximately 5-15% rel. efficiency present in relative terms a much larger Compton background than larger detectors do. The parameter peak-to-Compton (PTC) ratio is a quality factor that serves as a guide to the desired performance, but parameters such as the material and thickness of the detector front window, end cap, and mount cup characteristics are nearly as important. Detectors with 20-35% rel. efficiency are optimal for fallout measurements in affected areas up to dose rates of 10-20 µSv/h. Smaller detectors tend to suppress the full energy peaks of important radionuclides, such as ^{137}Cs, due to lower photo peak efficiency and smaller PTC ratio. When quantifying low activity levels or searching for sources with an unknown location, bigger detectors are preferable.

In Papers I-IV, the use of HPGe detectors for PTV measurement applications was investigated.

In Paper II, the characteristics of an HPGe detector were investigated in relation to the PTV ratio and the origin of valley counts. An ORTEC GMX series n-doped, beryllium-windowed HPGe detector with an efficiency of 18% (see Table 1) was selected in a study attempting to match Monte Carlo calculations performed in MCNP5 (Los Alamos National Laboratory) with measurements made under the most optimal circumstances that could be presented. The physical dimensions of the detector and its components were estimated using medical diagnostic tools (CT and flatbed X-ray) and radioactive sources for scanning to give the best input to the Monte Carlo model as possible. The detector crystal was mounted by 4 Teflon screws pressing the crystal to one side of the mount cup, resulting in the detector being off-

center by a few millimeters. The detector was placed in a low background counting (LBC) room, which presented almost negligible pulse counts from the background in the setup compared to the source count rate. The detector front window consisted of 0.5 mm of beryllium, presenting almost no attenuation of the primary ^{137}Cs gamma photons (662 keV). However, the other nearby structures surrounding the detector, such as the detector mount cup, may cause scatter that could be registered in the ^{137}Cs valley.

In Paper III, several HPGe detectors were tested to investigate how the ^{137}Cs PTV ratio differs between detectors. With the 30 keV valley interval mentioned in section 1.2, the difference between a small and large HPGe detector was less than anticipated (26% vs. 123% rel. efficiency). The reason was determined to be the higher ability of the larger detector to fully absorb the 662 keV photons (i.e., the higher PTC ratio). Furthermore, the PTV ratio of the small n-type detector was also in agreement with that obtained for small and large p-type detectors. This observation simplifies the use of the PTV method, as which detector is available in a given measurement situation appears to be of less importance.

2.2 Monte Carlo calculations

In Papers II and III, Monte Carlo simulations were used as a tool to investigate internal characteristics that cannot be described without destroying the function of the detector. Monte Carlo code MCNP5 (Los Alamos National Laboratory) was used to understand the influence of detector parameters, such as dead layer thickness, and the importance of Ge crystal positions relative to surrounding structures. This work was done based on a MSc thesis (Kock, 2007) that provided initial experience in the compliance between the measured full energy counting efficiency of the detector and the calculated efficiency using MCNP5. The efficiency values differ when using manufacturer-specified dimensions, and present a calculated rel. efficiency value that is higher than the measured value. When modeling a p-type HPGe detector, the dead layer (contact) is on the outside of the Ge crystal, which in practical terms is a shell of inactive germanium. An often-used approach in Monte Carlo calculation of p-type detectors is to increase the thickness of the dead layer until an agreement is reached between the measurement and calculation. To compensate for the difference in detector efficiency, there is the possibility of changing the active detector volume in the model by changing the thickness of the dead layer. A small change in the thickness of the dead layer for a p-type detector makes a significant difference in the absolute peak efficiency for ^{137}Cs. This approach is dependent on the setup having one or a few full energy peaks with roughly the same photon energy to optimize. When a setup contains several gamma energies in a broad energy range, it is not

possible to have one optimized model of the measurement setup in agreement with all situations.

When n-type HPGe detectors are used, one has to bear in mind that the dead layer is on the inside of the contact hole of the coaxial detector (see Figure 4 and Figure 20, upper right image). For higher photon energies (>500 keV), a small increase in the inner dead layer will not significantly affect the full energy peak efficiency. To obtain an effect that corrects for the higher simulated efficiency value compared to the measured efficiency, an unreasonably thick dead layer has to be applied to the model. This causes a problem when the full energy peak efficiency is the main focus, but it can be addressed by using an energy factor. The factor corrects the full energy peak efficiency to the measured value. When the aforementioned geometric correction is applied to the detector model by increasing the dead layer thickness, the increased dead layer produces more scattered photons. These scattered photons will be registered in the valley by the detector. The increase of dead layer thickness will affect both the peak and valley simultaneously. Therefore, matching the model with regards to both the full energy peak and valley net counts is a more sensitive operation than usual for both detector types, but much more so for the n-type detectors. One other way to optimize the model for n-type detectors is to fill the inner contact hole of the detector with an unreasonably thick inner contact pin for charge collection (red pin within the blue germanium crystal in Figure 4). This, of course, is not a true description of the detector; the inner contact pin is not a homogeneous metal rod and it does not fill the inner hole of the detector completely. An example of a contact pin can be seen in Figure 4 and 20 (upper left image). However, this was one way of optimizing the model to obtain a closer match to the measurements.

In Paper III, MNCP5 was used to estimate the contribution from photons scattered in air to be registered in the valley for a detector at 1 m measurement height with photons originating from source distances between 2.5 m and 17.5 m. The measurement setup was made to investigate the ^{137}Cs PTV ratio with respect to different incident angles (i.e., different source to detector distances). These calculations were essential, as there were no sufficiently strong sources of the "scatterless" type available for purchase, and it would be difficult to find suitable terrain with good enough characteristics. The calculations served as an indication of how the incident angles from farther away would affect the obtained PTV ratio.

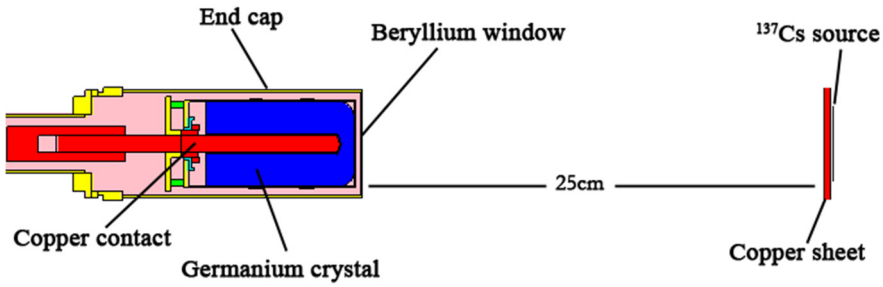

Figure 4.
The measurement and detector configuration simulated in Paper II.

2.3 Statistical calculations of the uncertainty of the PTV ratio in a single full energy peak pulse height distribution

The statistical uncertainty of the PTV ratio for ^{137}Cs of the measurements in the LBC room was evaluated.

The gross counts in the peak (P_G) and valley (V_G) ROI can be expressed as:

$V_G = V_{Cs} + V_{B,Cs}$ and
$P_G = P_{Cs} + P_{B,Cs}$

The PTV ratio measurement was obtained during a time interval of t_{Cs} and the background counts during a time interval of t_{bkg}. Thus, the PTV_{Max} ratio expression can be written as:

$$PTV_{Max} = \frac{P_{Cs}/t_{Cs}}{V_{Cs}/t_{Cs}} = \frac{(P_G - P_{B,Cs})/t_{Cs}}{(V_G - V_{B,Cs})/t_{Cs}}$$

Where PTV_{Max} is the maximum PTV ratio, i.e. when the measurement setup provides minimal scattering material between the detector and the source. The peak and valley background can be expressed as:

$$P_{B,Cs} = \frac{P_B}{t_{bkg}} = P_B \cdot (t_{cs}/t_{bkg}) \text{ and,}$$

$$V_{B,Cs} = \frac{V_B}{t_{bkg}} = V_B \cdot (t_{cs}/t_{bkg})$$

Where P_B and V_B is the total background in the peak and background ROI respectively, adjusted for the event of non-equal measurement time between the PTV_{Max} measurement and the measurement estimating the background.

This gives the following expression for the maximum PTV ratio:

$$PTV_{Max} = \frac{(P_G - P_B \cdot (t_{cs}/t_{bkg}))}{(V_G - V_B \cdot (t_{cs}/t_{bkg}))}$$

When estimating the variance of PTV_{Max} (which is a ratio)

$$\sigma^2(a/b) = \left(\frac{\sigma^2(a)}{a^2} + \frac{\sigma^2(b)}{b^2}\right) \cdot \frac{a^2}{b^2}$$

$$\Leftrightarrow$$

$$\frac{\sigma^2(a/b)}{(a/b)^2} = \frac{\sigma^2(a)}{a^2} + \frac{\sigma^2(b)}{b^2}$$

When applied to the PTV_{Max} equation this means that

$$\frac{\sigma^2(PTV_{Max})}{PTV_{Max}^2} = \frac{\sigma^2(P_G - P_B \cdot (t_{cs}/t_{bkg}))}{(P_G - P_B \cdot (t_{cs}/t_{bkg}))^2} + \frac{\sigma^2(V_G - V_B \cdot (t_{cs}/t_{bkg}))}{(V_G - V_B \cdot (t_{cs}/t_{bkg}))^2}$$

$$\Leftrightarrow$$

$$\frac{\sigma^2(PTV_{Max})}{PTV_{Max}^2} = \frac{\sigma^2(P_G) + \sigma^2(P_B \cdot (t_{cs}/t_{bkg}))}{(P_G - P_B \cdot (t_{cs}/t_{bkg}))^2} + \frac{\sigma^2(V_G) + \sigma^2(V_B \cdot (t_{cs}/t_{bkg}))}{(V_G - V_B \cdot (t_{cs}/t_{bkg}))^2}$$

In the above expression the term (t_{cs}/t_{bkg}) can be viewed as a constant, with negligible uncertainty, resulting in the following expression:

$$\frac{\sigma^2(PTV_{Max})}{PTV_{Max}^2} = \frac{\sigma^2(P_G) + \sigma^2(P_B) \cdot (t_{cs}/t_{bkg})^2}{(P_G - P_B \cdot (t_{cs}/t_{bkg}))^2} + \frac{\sigma^2(V_G) + \sigma^2(V_B) \cdot (t_{cs}/t_{bkg})^2}{(V_G - V_B \cdot (t_{cs}/t_{bkg}))^2}$$

Using the Poisson statistics, $\sigma^2(a) = a$, when $a \in \mathbb{P}oisson$. This further develops the expression of the uncertainty to:

$$\frac{\sigma^2(PTV_{Max})}{PTV_{Max}{}^2} = \frac{P_G + (t_{cs}/t_{bkg})^2 \cdot P_B}{(P_G - P_B \cdot (t_{cs}/t_{bkg}))^2} + \frac{V_G + (t_{cs}/t_{bkg})^2 \cdot V_B}{(V_G - V_B \cdot (t_{cs}/t_{bkg}))^2}$$

$$\Leftrightarrow$$

$$\sigma(PTV_{Max}) = \sqrt{\frac{P_G + (t_{cs}/t_{bkg})^2 \cdot P_B}{(P_G - P_B \cdot (t_{cs}/t_{bkg}))^2} + \frac{V_G + (t_{cs}/t_{bkg})^2 \cdot V_B}{(V_G - V_B \cdot (t_{cs}/t_{bkg}))^2}} \cdot PTV_{Max}$$

Finally, the terms can all be estimated from measurements. If then applied to a typical LBC room measurement with

P_G =70 325 counts
P_B = 410 counts
V_G =2109 counts
V_B =142 counts
$(t_{cs}/t_{bkg}) = 1$
$PTV_{Max} = 45.1$

The total estimated uncertainty of the PTV ratio would be
$\sigma(PTV_{Max}) = \pm 1.3$, which means a relative uncertainty of approximately 2.9 %.

2.4 Measurement geometries

2.4.1 Laboratory and experimental setups

Different facilities, setups, and sources were used to investigate the components in the detectors and the geometry that influences the PTV ratio as described later in this section. When investigating the origin of scattered source photons, testing should be performed in an environment with as low a background as possible. The preferable choice is to work in a LBC room. The university hospitals in Lund and Malmö operate such facilities, and both have been used in this thesis. The typical outdoor background count rate over the energy range 30 to 3000 keV *in situ* in the south of Sweden for a 26% HPGe detector is approximately 400 cps, and the typical count rate inside a LBC room is 1 to 5 cps. The typical reduction of the background count-rate in the Lund and Malmö LBC rooms is a factor 100. There was little difference

between the facilities in general, except during rainy weather. The rain affected the Lund LBC room by increasing the background count rate due to the atmospheric washout of natural uranium series daughters and ^{7}Be. The Malmö LBC room is located on the 6th floor to effectively avoid this effect. The sizes of the facilities are different, with the LBC room in Malmö being larger and offering more possibilities to house a variety of more space-consuming measurements involving angular measurements and close to "free in air" setups.

The accuracy at which the PTV can be determined experimentally for a given source detector set-up, is related to the measured peak and valley counts above the background counts. To further investigate the PTV ratios of different incident angles from a point source either on top of or in the ground, a scaled down PTV ratio experiment was performed. The ground beneath the detector was leveled off using a thick layer of sand. The experimental frame supporting the detector did not interfere with the experiment. The same frame setup was also used in Japan *in situ*, and is shown in Figure 5.

Figure 5.
PTV measurements close to the fence of the Fukushima Daiichi reactor site in 2013 using a thin steel frame to cause minimal obstruction of the $^{134, 137}$Cs photon field.

The source used was of a type commonly described as scatterless, meaning that the encapsulation is the thinnest possible while still being thick enough to encapsulate the radioactive source material (Eckert&Ziegler Isotope Products). These sources are available up to approximately 3.7 MBq, which limits the dimensions of the

experiment setup to a few meters with the source positioned 2 cm in the ground. Therefore, to mimic distances beyond 2.5 m, the detector was lowered closer to the ground to match the incident angle of a source farther away. Consequently, this setup did not fully include air scatter, which increases with larger source to detector distances. The setup was intended to increase understanding of the scatter contribution caused by the soil in order to further understand and refine the PTV method and its use.

To understand the influence of other radionuclides with higher photon energies when employing the PTV method *in situ* for ^{137}Cs, a measurement setup for ^{134}Cs and ^{137}Cs utilized a vertical steel mast. The two radionuclides were positioned at different distances from the detector to simulate different ^{134}Cs:^{137}Cs activity ratios. The intention with the experiment was to find a way to determine the effect of ^{134}Cs on the ^{137}Cs valley, and perhaps find a simple way to compensate for potential effects. The experiment had to use a steel encapsulated ^{137}Cs point source to achieve the desired ^{134}Cs:^{137}Cs activity ratios. The steel encapsulated source generated a slightly lower PTV_{Max} compared to a scatterless source, but no more than 10%. Prior tests evaluated the differences in PTV ratio with a ^{137}Cs source at several distances, from close to the detector up to several meters.

2.4.2 In situ measurements - searching sources in Republic of Georgia

In the Republic of Georgia, mobile measurements and stationary PTV ratio measurements were performed for both scientific and radiation safety purposes. Georgia has had difficulties with abandoned sources since the fall of the Soviet Union, and campaigns have been conducted to improve the situation. Casualties and critical injuries have been reported due to misplaced HASS sources, such as radio thermal generators (RTGs) (IAEA, 2014). Actions were performed to increase radiation safety. The visited site was an old ground level repository (Radon type) storing an unknown quantity of radioactive waste (Abramenkovs, 2006).

Figure 6.
Map overview of the repository site in Georgia. The dark contour is the outer perimeter fence.

The initial task was to find and locate a high activity ^{60}Co radiotherapy source, which should be at the site but could have been buried outside the repository in 1995. The region, including the site, was mountainous terrain 45 km outside Tbilisi without electricity, cell phone reception, or other necessities. The visit demanded proper planning and external base support (EBS) in Sweden for efficient evaluation of the measurements. The 123% HPGe detector (Table 1) was used to map the repository, and the PTV method was used to complement all other investigation methods.

No traces of a high activity ^{60}Co radiotherapy source were found when performing a survey of the site outside the repository using the $LaBr_3$(Ce) and 123% HPGe detector. Instead, ^{137}Cs and ^{60}Co were found in the center of the repository. Additional point sources were found close to the shed. The radionuclides were identified as ^{108m}Ag and ^{152}Eu, and both of the sources were weak sources, about 20 kBq and 80 kBq respectively (Figure 7).

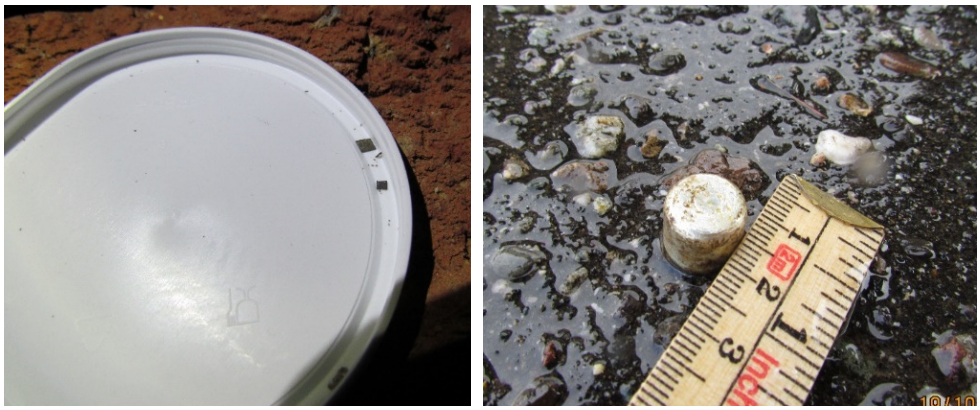

Figure 7.
The picture to the left shows the two ^{108m}Ag point sources found in the dirt by the old shed, and they are about 2 mm in dimension. The picture to the right shows the ^{152}Eu found behind the shed under the grass surface.

2.4.3 The use of the PTV method (outside Paper I).

In order to more thoroughly investigate the inventory of the repository and to test the PTV method, spectrometric measurements useful for evaluating the PTV ratio were performed in a 1 m × 1 m grid over the part of the repository not covered by 1 m of soil. The part covered by soil (top left in Figure 8) showed no evidence of containing sources of interest. The measurement time for each grid measurement was set to 600 s live time for each measurement, and the detector was moved along the lines indicated in Figure 8. During all grid measurements the detector was positioned just above the concrete lid and distanced using a 2-cm-thick plastic foam pad. The grid measurements presented 45 measurements in total, and the analysis was later focused on the evaluation of ^{60}Co and ^{137}Cs.

Figure 8.
A Photograph of the PTV ratio measurement grid and radionuclide mapping of the radioactive waste (Radon type) repository. The grid was constructed with white markings on the ground in combination with a tape measure.

A rupture in the lid of the repository was discovered during the work in the top right end of the grid, offering the opportunity to photograph some of the repository content (see Figure 9).

Figure 9.
A small part of the repository content. This photograph show used smoke detectors containing either ^{226}Ra or ^{241}Am partly covered in soil and water.

The PTV ratio was used with inverse square law calculations in an attempt to position the sources in the repository. The PTV ratio, peak intensity, and the ratio between the valley ROI and background ROI were plotted in a grid in a spreadsheet. The PTV ratio could serve as an indicator of the burial depth of the source. The idea of the ratio between the valley and background ROI was that it would indicate whether the valley count rate increased sufficiently above the background ROI and present a credible PTV ratio. The peak intensity was plotted as an interpolation image to support the conclusions about the positioning of the activity of the two radionuclides and to make comparisons with the spreadsheet results. The ^{60}Co in the repository perturbs the ^{137}Cs PTV ratio via scattered Compton photons. The amount of disturbance is dependent on the ^{60}Co burial depth. However, the Compton distribution has a fairly even slope over the peak and valley (see Figure 10).

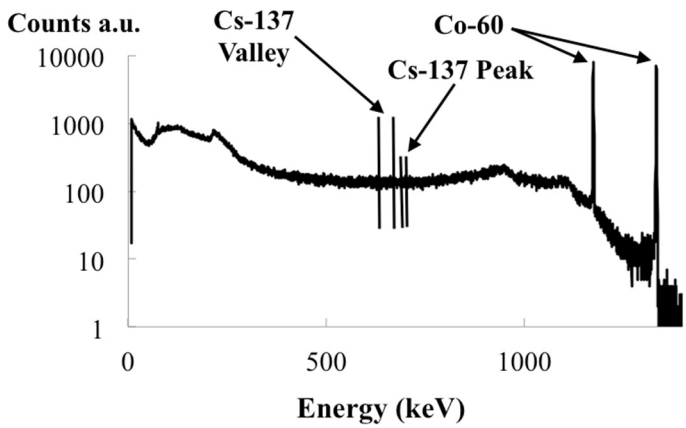

Figure 10.
A ^{60}Co pulse height distribution with the ^{137}Cs peak and valley ROI marked. The contribution to the ^{137}Cs valley ROI by ^{60}Co is approximately the same on both sides of an full energy peak at 662 keV.

2.4.4 *In situ* measurements - estimating the fallout outside Fukushima Daiichi

The two smaller HPGe detectors (Table 1) were brought to Japan in three IAEA RANET workshops conducted in the restricted zone outside the Fukushima Daiichi nuclear power station between 2013 and 2016. The primary purpose of the visit was to perform inter-comparison measurements to evaluate detectors and calibrations used for estimating deposition (Bq/m^2), at different locations inside the restricted zone. The activity levels presented a challenge to the equipment and evaluation, rising well above 3 MBq/m^2 ^{137}Cs in total deposition at a few locations close to the Fukushima nuclear power station (Saito et al., 2015, see Figure 11).

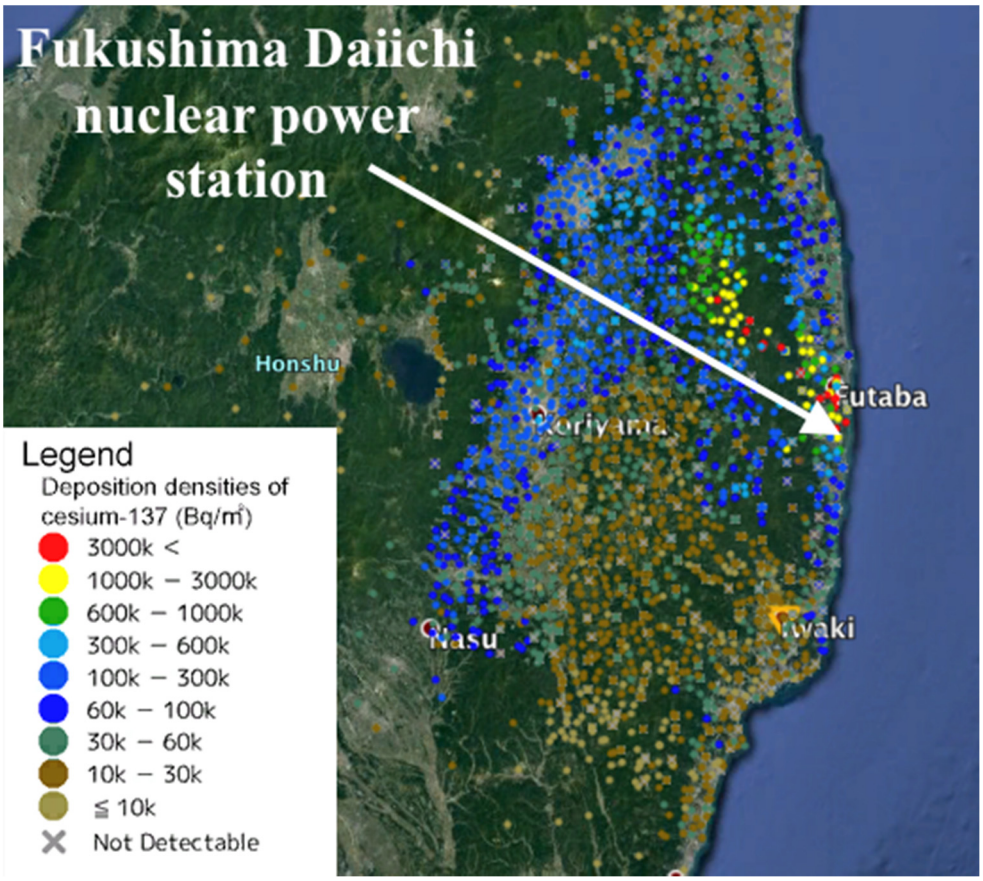

Figure 11.
2011 deposition density map (Bq/m^2) of ^{137}Cs based on sampled points outside the nuclear power station in the Fukushima Daiichi region (JAEA public material, www.jaea.go.ip/emdb/en/portals/b211/).

The surveys presented a unique opportunity to perform a large number of PTV ratio measurements at many locations for scientific purposes. Pulse height distributions from the two detectors were used in this thesis with a focus on the PTV ratio and the feasibility of the method in actual fallout situations. The estimated values for deposited ^{137}Cs varied between 0.1 and 8 MBq/m^2 using a surface calibration model (see Paper IV). The ^{134}Cs:^{137}Cs activity ratio was reported to be 1:1 during the reactor accident in Fukushima Daiichi in 2011 (UNSCEAR, 2013). Due to the passage of time since the release of radioactivity, the amount of ^{134}Cs decreased from the expected and measured ^{134}Cs:^{137}Cs ratio of 1:2 at the first visit in 2013 to 1:4.5 during the last visit in 2016.

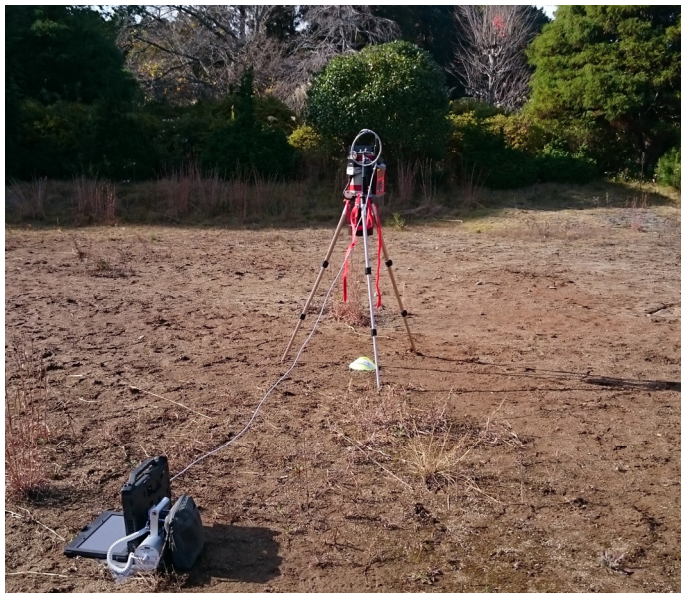

Figure 12.
Typical measurement geometry in Fukushima prefecture outside the Fukushima Daiichi nuclear power station in 2015, where measurements were performed at a sports field with as flat a ground surface as possible within the field of view of the detector. The collimator was applied to the detector and is visible hanging in the red straps.

Figure 13.
The collimator used in Paper IV applied to the detector, limiting the field of view to a radius of approximately 6 m.

There are other *in situ* parameters, such as high count-rate effects, variations in the spatial distributions of the deposition, and surface roughness, among others that need to be handled in order to estimate the amount of cesium radionuclides at the measurement location. It is important to bear in mind that these locations can never be treated as a validation or calibration of any setup, because the exact source configuration in terms of total surface deposition and ground penetration was not known. However, the restricted zone outside Fukushima Daiichi offers an opportunity for relative comparisons between different locations with support from other investigations, such as distribution mapping (Figures 12-14).

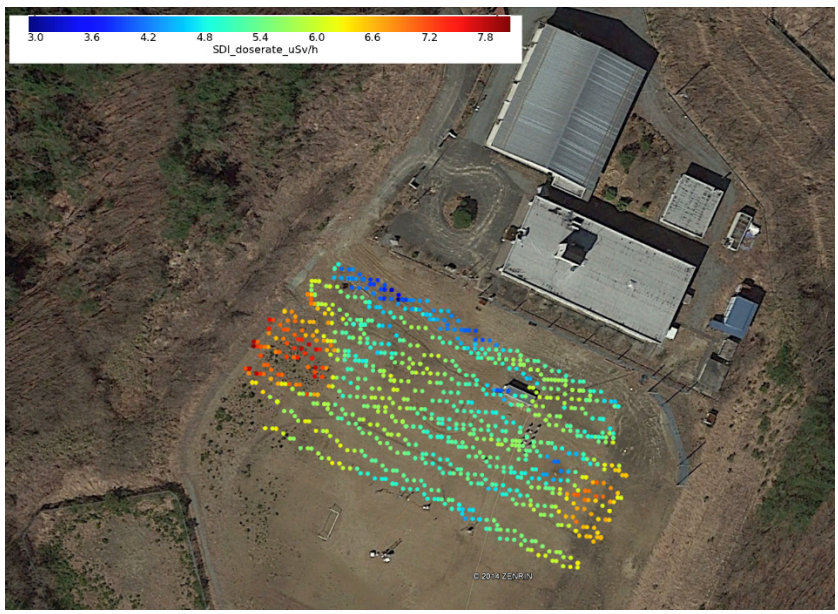

Figure 14.
Detailed mapping of an undisturbed yard outside the Fukushima Daiichi site. The variations in deposition are obvious and a more a rule than an exeption.

3. Results and discussion

3.1 Paper I

The preparatory point source field experiments in Sweden showed that the 123% HPGe detector (see Table 1) was superior in detecting the ^{137}Cs sources (activities ranging from 54 kBq to 570 kBq) both on the ground surface and buried 5 cm under the ground surface. The $LaBr_3$(Ce) detector was similar in detection efficiency to the NaI(Tl) detector, despite the higher energy resolution and higher intrinsic efficiency of the $LaBr_3$(Ce) detector. The lack of advantage for the $LaBr_3$(Ce) detector over NaI(Tl) in this survey could be the effect of the low background of the site chosen for the testing, as well as the internal contamination of the detector. When encountering a higher background, the $LaBr_3$(Ce) detector will probably outperform the NaI(Tl) detector due to the difference in signal-to-noise ratio and scintillation characteristics.

The weight of the HPGe-based backpack system is an issue when considering the physical workload of the operators using the system. However, when searching for weak sources, there are few if any other options for performing measurements to clear an area. The system can be optimized to weigh less but will never reach the mobility and portability of scintillation detectors of a similar size.

The EBS function explored in Paper I proved to be an efficient way of operating in time-limited and high-workload missions. The possibility of making proper decisions is heavily degraded by the circumstances during missions such as this, with a combination of few sleeping hours and physically greater workload than normal. Therefore, the EBS function freed up valuable time on site, which is otherwise often used for evaluation.

The discovered sources did not include the requested ^{60}Co source. However, the findings of ^{152}Eu and two ^{108m}Ag (at one position) sources validate the sensitivity of the HPGe backpack system and the effectiveness of the EBS function. The localization of the spots contaminated with ^{226}Ra and ^{137}Cs further indicates the reliability of the system used (the mobile measurements in combination with EBS function) in terms of the detection capability of weak radioactive sources positioned within an abnormally high anthropogenic background. The HPGe detector also has drawbacks in the backpack configuration because it is sensitive to microphonic noise created by bushes, trees, and other hard objects that bounce against the liquid

nitrogen dewar. When these hits occur, it induces vibrations, increasing the count rate and potentially creating false-positive source alarms in the selected ROIs. The findings in close vicinity to the repository are difficult to compare to other studies within the same field of research, as the environment in which the measurements were performed differ (Cresswell and Sanderson, 2012). There is also reason to believe that one or several other weak sources are still present *in situ* at the repository site because the limited time did not allow the team to thoroughly evaluate all positions indicated by the EBS analysis.

The measurements revealed an applicability of the PTV method in combination with other methods in localizing a source buried in the ground. The additional information gained by the PTV ratio measurements strengthens the conclusions on source position, i.e. the burial depth. The PTV ratios for ^{137}Cs in the grid measurements are shown in Figure 15.

Figure 15.
^{137}Cs PTV ratio values measured in the 1 m × 1 m grid in Georgia, at a measurement height just over the repository lid, with a 2-cm-thick rubber pad between the repository and detector.

The PTV ratios marked in red in Figure 15 indicate a shallow buried source. Compared to the results of buried sources in Figure 16, this is misleading. The PTV ratios indicate a source buried underneath a couple of centimeters of soil or concrete, despite the concrete lid of the repository being 15 cm thick.

Figure 16 illustrates the interpolated relative ^{137}Cs peak count rate over the repository. One location with a high PTV ratio coincides with the high peak intensity of ^{137}Cs and the source is likely found just below the concrete lid. The results shown in Figure 22 (Section 3.3) indicate a burial depth of a few cm for the red PTV ratios in Figure 15, which is not possible. There are other positions with high PTV ratios, but none with an evidently high ^{137}Cs peak. This could be ascribed to perturbation of the ^{137}Cs PTV ratio by other radionuclides in the repository or a dispersed source. As an example of the ^{60}Co perturbation, the relative peak intensity of ^{60}Co is presented in Figure 16. The contribution from ^{60}Co overlaps with ^{137}Cs.

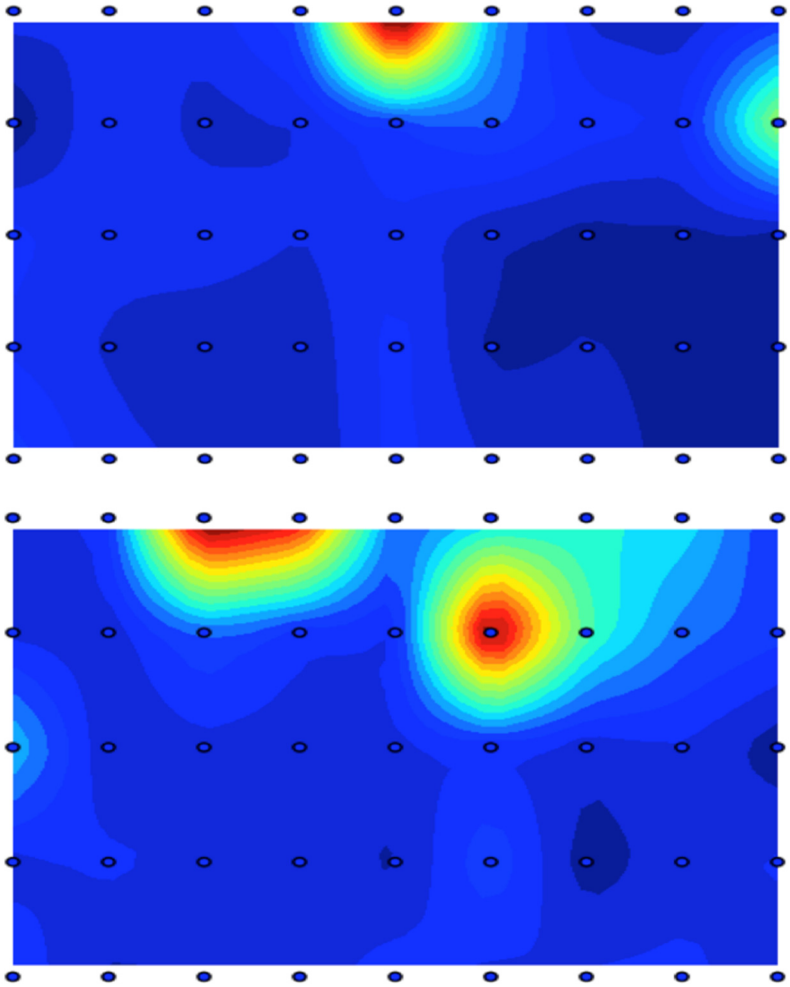

Figure 16.
Interpolated image of the ^{137}Cs net peak count rate (top) and the ^{60}Co net peak count rate (low) obtained from the repository in 1m × 1 m grid measurement positions (blue circular dots in the illustration). Illustrations made by Jonas Nillson, co-author of Paper I.

There are several positions in Figure 15 that present too high ^{137}Cs PTV ratios considering the lid thickness. When combining the ^{137}Cs relative peak count rates with the PTV ratios, one high PTV ratio in Figure 15 coincide with the maximum intensity in the plot in Figure 16. A test was performed to determine whether the ^{137}Cs PTV ratio, and specifically the counts in the valley, could be trusted to be true valley counts. One can compare the gross valley counts with the counts in the background ROI to the right of the full energy peak at 662 keV (Figure 17).

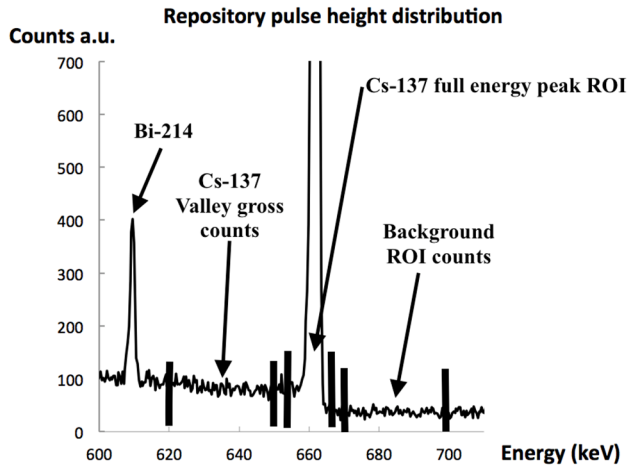

Figure 17.
A authentic repository pulse height distribution visualizing the valley gross counts, the full energy peak ROI, and background ROI.

When plotting the ratio between the gross valley counts and the background ROI counts (see Figure 18), one can easily come to the conclusion that, if this "new" ratio is close to 1, the PTV ratio has high statistical uncertainty. Adding this information to the complete evaluation of source localization may give further guidance of the specific source position as illustrated in the following example.

5.8	2.2	1.6	2.2	6.2	1.5	1.3	1.5	1.7
13.4	3.3	3.1	2.3	2.0	1.6	1.5	1.6	1.6
1.2	1.3	1.3	1.5	1.5	1.7	1.7	1.7	1.6
1.2	1.2	1.2	1.2	1.5	1.3	1.4	1.5	1.3
1.2	1.2	1.2	1.2	1.5	1.3	1.6	1.7	1.6

Figure 18.
The ratio between the valley ROI and background valley ROI obtained in the the 1 m × 1 m grid measurements.

The idea is that the reliability of the PTV ratios could be assessed by looking at what positions exceed the value 2 in "the valley to background ROI ratio" (Figure 18). If these positions are colored green, the positions could supply information about where not to discard the PTV ratio, and thus make further investigations (Figure 19).

If the PTV ratio indicates a shallow burial depth and the ratio between the valley and background ROI is above 3, the suggestion is that the PTV ratio can tentatively be trusted. If all of the results obtained from measurements at the repository are combined (highest intensity spot, PTV ratio, high ratio between gross valley counts and background valley counts), a source location could be established to a higher degree of certainty. Still, the results appear unreliable, but there is a slight possibility that the lid could be flawed, which was a parameter out of control. Together with an analysis of the valley slope, the ^{137}Cs PTV ratio reliability may be further improved.

1.7	2.3	6.2	14.9	17.8	13.1	9.3	10.2	12.0
1.6	1.9	3.4	6.7	12.1	11.4	7.9	14.9	14.7
3.8	8.1	7.4	5.7	13.8	12.8	17.0	14.4	14.5
4.5	9.3	6.9	2.6	13.2	9.3	10.5	12.0	10.4
6.9	8.3	9.2	5.6	12.5	10.7	11.5	9.9	7.7

Figue 19.
The PTV ratios with a significant valley count (i.e., >2 for the valley to background ROI ratio) are colored green in the figure.

3.2 Paper II

3.2.1 LBC room measurements

When comparing two different valley ROI settings using the measurements made at the LBC room, a 30 keV valley would fit between the natural 609 keV ^{214}Bi full energy peak and the 651 keV single k-escape peak of germanium in the detector. In combination with the increased number of valley counts and the associated improvement in counting statistics, the broader valley ROI was chosen. The use of the scanning of a detector with a well-collimated ^{125}I photon-emitting source provides useful information on the internal physical characteristics of the detector. The diagnostic radiographic imaging modules (CT and planar X-ray) used in this paper provided useful information about the external structures outside the detector and, when combined, provided a complete picture of the detector and detector assembly.

3.2.2 MCNP5 simulated peak and valley contribution compared to measured count rates

The discrepancy in the observed and simulated full energy peak efficiency of 25% illustrates a fundamental problem when comparing results of measurements and simulated results. Although addressed in the literature (Gilmore, 2008; Marzocchi et al., 2010), there have been no specific and valid explanations that account for the magnitude in the discrepancies between measured HPGe detector results and Monte Carlo-simulated values. The simulated and measured valley counts show no difference when no obstructing material is present between the source and detector. On the other hand, the discrepancy increases with the introduction of copper scattering material between the source and detector. The scattered photons showed the same trend as the full energy photons (i.e., a higher detection efficiency of scattered photons in the detector compared to measurements). By increasing the detail of electron transport through materials in the models, the discrepancy was expected to decrease. Unfortunately, the opposite effect occurred and discussions with ORTEC personnel using MCNP5 (Los Alamos National Laboratory) and MCNPX (Los Alamos National Laboratory), as well as other experts, presented no solution to this issue.

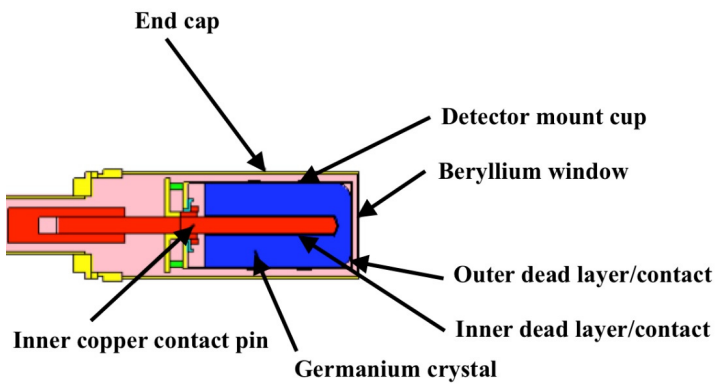

Figure 20.
Schematic illustration of different detector components. The thicknesses of the inner and outer dead layers differ with detector type (n, p). The p-type detector has the thick dead layer on the outside of the germanium crystal, where it is oriented on the inside of the n-type detector.

3.2.3 Significance of inner components for the PTV ratio

The central electrode geometry and its thickness are important for the "near detector" production of scattered photons ending up in the valley. The calculations show that, by increasing the diameter of the central electrode up to complete filling of the hole

in the Ge crystal, the valley counts increase and reduces the PTV ratio closer to the measured value (see Figure 8A in Paper II).

The inner and outer dead layer is not visible to the eye when looking at an actual germanium crystal (see upper right in Figure 21). Still, the thicknesses of the outer dead layer play an important role in in the detector internal production of valley counts. The dimension of the inner dead layer makes little difference when the thickness is within the range of the manufacturer specification for a nominal detector (see Table 2 in Paper 1 and Figure 20).

Figure 21.
A photograph of the central electrode (upper left), the germanium crystal bottom (upper right), the bulletized top (lower left), and the detector front face (lower right) of a disassembled 22% (rel. efficiency) ORTEC n-type PopTop^{tm} detector. The near perfect crystal structure surface and outer thin (0.6 µm) contact presents a mirror-like surface.

3.3 Paper III

3.3.1 The valley range, maximum PTV ratio, and incident angle dependence

The paper focuses on the measurements and practical aspects of using the PTV method. A comparison between the 20 keV and 30 keV valleys provided clarity to the effect this difference in valley range would imply. A narrower valley ROI increases the uncertainty of the obtained PTV ratio due to fewer counts in the valley. A broader valley ROI increases the possibility of disturbances. The maximum PTV ratio not only provides information about the maximum achievable PTV ratio for a detector, but also estimates the specific detector valley ROI background. The measurements in the LBC room contributed almost no natural background or air scatter. The valley counts are produced by single or multiple scatter in the air, the detector, and the material surrounding the detector. This provides an estimate of the number of detector inherent background counts in the valley, which was in the range of approximately 2.0 to 2.5% per detected photon in the full energy peak for ^{137}Cs according to the maximum PTV ratios presented in Paper III. The differences in maximum PTV ratio between large and small detectors and incident angles were more pronounced for the 20 keV valley. The choice of a 30 keV valley presents a more angle-independent PTV ratio between different detector types and sizes.

The most notable difference between a p-type and n-type detector is the location of the dead layer. The p-type detector is predestined to produce more detector-internal scatter (valley background) in the dead layer on the outside of the detector. This would result in a lower maximum achievable PTV ratio under optimal circumstances. However, the higher PTC value of the larger detectors seems to efficiently cancel out this effect, resulting in comparable PTV ratios to smaller detectors. When comparing the two smaller detectors of different type, one would expect a significant difference. There is a difference that is more prominent when using the 20 keV valley, but it is almost unnoticeable when using the 30 keV valley. This is positive for the user of the PTV method, i.e. the user has one thing less to care for. The results also indicated that detectors between 18 and 123% rel. efficiency are feasible regardless of detector size and type. However, this needs to be investigated further as only three detectors were used in this comparison. The positioning of the valley within a few keV from the valley range in this thesis (620-650 keV) generates a variation in ^{137}Cs PTV ratio of approximately 5%, which is low enough to allow the user to position the valley in the pulse height distribution at a suitable location between the full energy peaks of ^{214}Bi and ^{137}Cs. Furthermore, a 1 keV increase in the valley (to 31 keV) also resulted in a 5% difference in ^{137}Cs PTV ratio.

3.2.2 Simulating a surface source *in situ* and Monte Carlo investigation of air scatter component

The experiment was carried out to understand and learn how the PTV ratio changes with burial depth, incident angle, and source to detector distance. The available sources and experimental area combined with the precision in ground surface flatness limited the distance of measurements to 2.5 m. The result of testing PTV ratio consistency in relation to different distances showed that, at ≥1 m, the PTV ratio remains a constant value independent of source distance. However, at a closer distance it may not be reproduced correctly due to solid angle effects and the individual characteristics of the detector.

The setup does not replace a full-scale experiment, but serves as an indicator of which areas underneath the detector that are important when estimating the ground penetration depth.

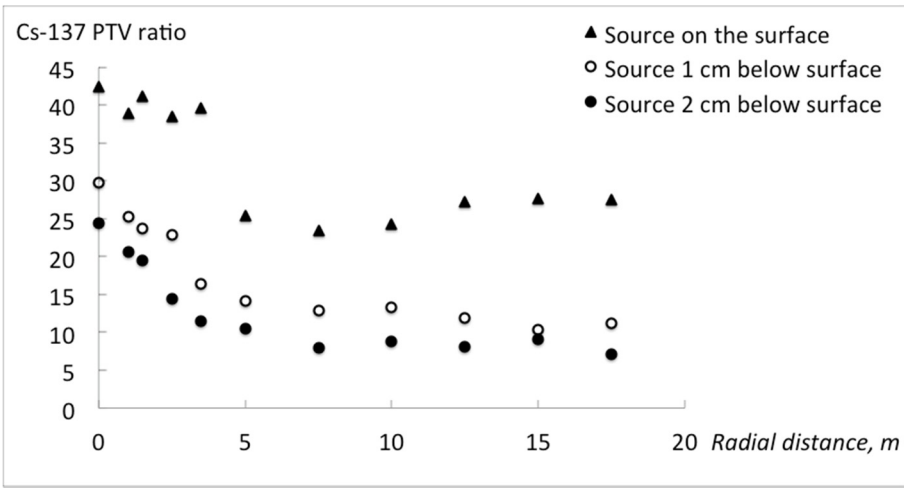

Figure 22.
The PTV ratio plotted against radial distance with the ^{137}Cs point source at the ground surface and buried in the ground 1 and 2 cm.

When the source is on the surface, the maximum PTV ratio of the current setup is achieved until the prolate scatter volume restricted by the allowed scatter angles for ^{137}Cs entered the ground (Figure 22 and Figure 23). Furthermore, the difference in PTV ratio when the source is buried 1 cm or 2 cm within a distance of 3 m allows the user to distinguish between a true surface source and a source that penetrates into the ground.

If one accepts larger incident angles (i.e., from buried sources), sensitivity in the ^{137}Cs PTV ratio in terms of describing the ground penetration will be lost. Large distances result in a significant amount of air scatter, and only source photons that interact in or close to the ground surface will be able to produce scattered photons that reach the detector. Because the experiment included simulated distances >2.5 m, simulations were performed in MCNP5 to estimate the air scatter contribution in relative terms for a source at the ground surface. In the current setup, the air scatter flux in the valley ROI energy interval was approximately 27% to 41% of the total valley energy flux at distances between 5 m and 17.5 m. This means that if the scatter in air is isolated and investigated separately, the air contribution to the valley energy flux increases substantially for farther distances. The test supported the conclusion that a field of view radius of 3 m is the optimal choice.

3.4 Paper IV

3.4.1 Collimators

Paper IV investigated whether a limitation to the field of view improves the estimation of fallout burial depth. The idea was taken from Paper III, in which the angular response in the ^{137}Cs PTV ratio was investigated, as well as the PTV ratios obtained when a point source was on the ground surface and buried 1 cm and 2 cm underneath the ground surface. Paper III (Figure 22) showed that, if the source is on the surface, it is possible to separate this surface source from a source further in the ground if the area under the detector is limited to a radius of approximately 3 m as measured on the ground (and with the detector 1 m above ground). Beyond 3 m, the prolate (elliptic) scatter volume (Figure 23) starts to intersect with the ground and the PTV ratio decreases with increasing distance.

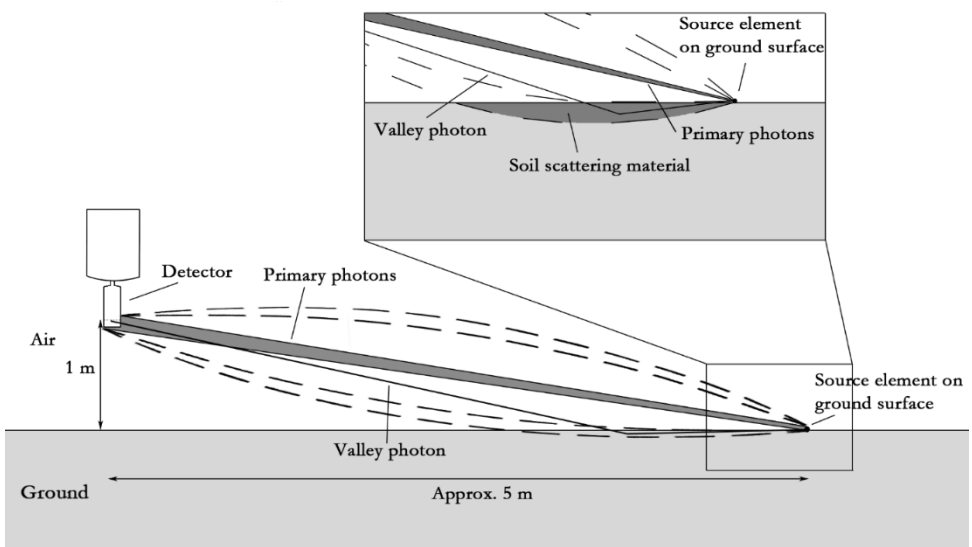

Figure 23.
Schematic overview of how the PTV ratio depends on geometry. Note that the scatter angles required for the scattered photon to end up in the valley intersect with the ground and decreases the PTV ratio with increasing radial distance.

These results indicate no additional gain from using a field of view that extends beyond 3 m in radius. At greater distances from the detector, the relationship is likely lost between the peak and valley that is supposed to express the penetration into the ground, as the path through the ground is significantly longer for a scattered photon with an origin farther away from the detector. In practice, this will "filter" out the possible valley photons, creating a changing PTV ratio at different radial distances from the detector. For the surface source, the variation is especially tricky. The PTV ratio is constant up to a distance of 3 m, and then decreases until the radial distance is enough to suppress the valley photons due to the process described earlier. At greater distances, the PTV ratio increases slightly again due to this loss of potential valley photons (see Figure 22).

To achieve a unique PTV ratio for a given burial depth, it is necessary to apply collimation to the detector. This would allow an estimation of burial depth in other applications, such as estimating an efficient burial depth for radionuclides in walls and other structures for decommissioning purposes.

3.4.2 Measurements outside Fukushima Daiichi

With the findings in Paper III, especially the results regarding limiting the field of view, measurements inside the restricted zone in Fukushima resulted in a number of

important experiences. Introducing collimation *in situ* to discriminate the incident angles from further distances increased the ^{134}Cs PTV ratio. The presented field of view had a radius of approximately 6 m based on the maximum incident angle of 80° and somewhat smaller than "normal" *in situ* field of views presented by others (Tyler et al., 1996; Boson et al., 2009). The collimation was expected to increase the PTV ratio for both ^{134}Cs and ^{137}Cs because larger incident angles were excluded. However, for ^{137}Cs there was no significant increase in the PTV ratio, and there could be many reasons for this. It could be an effect of the collimator itself or the scatter contribution in the ^{137}Cs valley from higher energy peaks in the pulse height distribution. Collimation appeared to increase the PTV ratio for ^{134}Cs at all locations (factor of increase: 1.19±0.03 (1SD)), but the ^{137}Cs PTV ratio did not follow the same trend (1.04±0.02 (1SD), Table 2).

Table 2.
PTV values from uncollimated and collimated measurements obtained in the Fukushima Daiichi region (Figure 12 and 13).

		PTV ^{134}Cs		PTV ^{137}Cs	
Location	**Type of surface**	**Open**	**Collimated**	**Open**	**Collimated**
1	Sand	17.0	19.0	13.5	14.5
2	Grit	13.9	16.9	12.6	12.7
3	Grit	13.5	16.2	11.7	11.7
4	Grit	13.8	17.1	12.7	13.5

The un-collimated mean ^{137}Cs PTV ratio was 10.7 ± 18% (1SD) for all types of surfaces. Because the measurements were made at a variety of different ground types, a difference between grass fields and asphalt was anticipated to be more than the achieved 10%. However, ^{134}Cs presented a more pronounced variation in PTV ratio compared to ^{137}Cs for the same locations. The difference between the ^{134}Cs and ^{137}Cs PTV ratios is prominent, ranging from 25 to 50% for the same measurement in many of the locations (Tables 2 and 3). The maximum ^{134}Cs scatter angle when calculated with Eq. 3 is approximately 12°. This is a 40% smaller scatter angle than for ^{137}Cs and allows for a larger field of view without the prolate scatter volume intersecting the ground surface.

A sports field in one of the contaminated areas outside Fukushima Daiichi was measured with an un-collimated detector before and after cleanup (Figures 24 and 25). The ground was covered by 5 cm of clean sand and the dose rate decreased approximately 90% (decay corrected) to 1.7 μSv/h. The PTV ratios of both cesium radionuclides decreased and maintained the internal ratio between them at approximately 2 (9.7 for ^{134}Cs and 5.4 for ^{137}Cs).

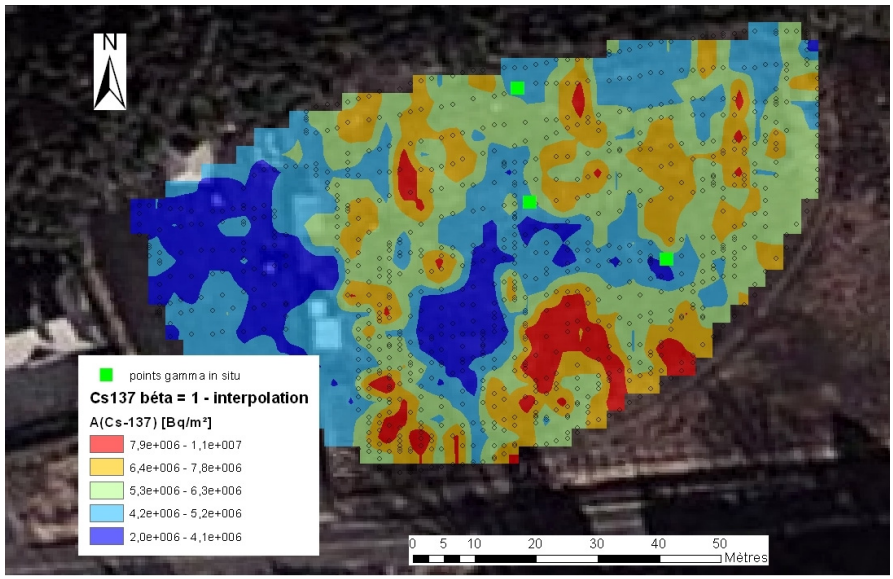

Figure 24.
The sports field outside Fukushima Daiichi mapped with mobile detectors before cleanup. The interpolated image displays the deposition (Bq/m^2). The points of measurement are within the colored interpolated distribution of cesium radionuclides (reproduced with permission from IRSN, France). The three green markers represent dose rate and *in situ* measurement positions with a dose rate of 25-30 µSv/h.

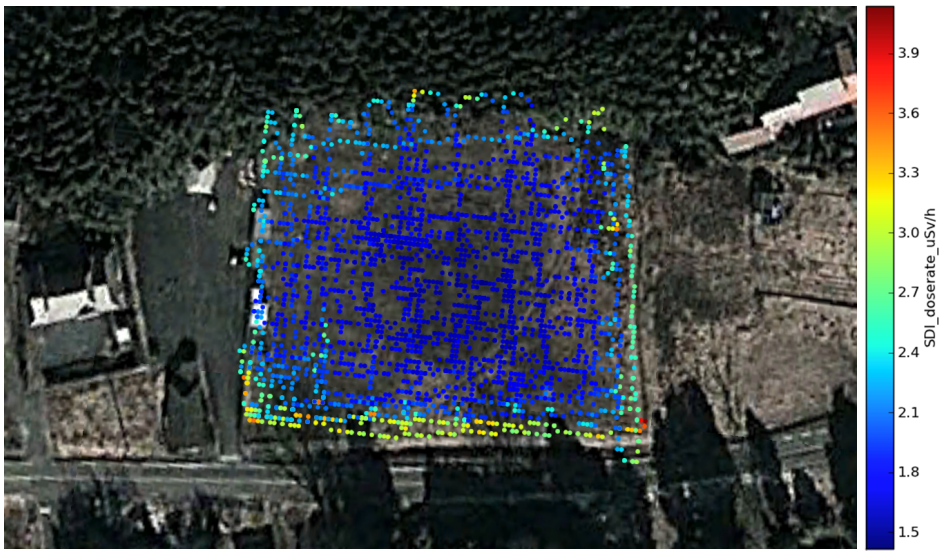

Figure 25.
Dose rates are represented as colored dots describing the SDI (Psectrum Doserate Index) dose rate in each location. The surveyed area is the same sports field as in Figure 24, and the measurements were made after cleanup operations.

When viewing the PTV ratios of the sports field and visualizing them relative to penetration depth, the different PTV ratios describe different source depths, which is an evident observation of perturbation. However, if the ^{137}Cs PTV ratios were compared to the results in Paper III, the value of the ^{137}Cs PTV ratio would be closer to 7 if the source is buried underneath 5 cm of clean sand. With the 10% increase (Paper IV) in PTV ratio originating from the comparison between the maximum PTV ratios of ^{134}Cs and ^{137}Cs, this value should be close to 8 for ^{134}Cs, which is just somewhat lower than the value of 9.7 presented in Table 3. In this context it is reasonable to believe that the clean layer of sand in some locations could either be less than 5 cm or more as well.

An interesting finding is the possible cleanup efficiency described by the SDI dose rate in Figure 25. The green markers in Figure 24 represent dose rate and *in situ* measurement positions, with a dose rate of 25-30 µSv/h. The near 90% reduction over the entire cleaned surface shows what can be achieved in limited areas when cleaning up after a nuclear accident.

Table 3.
PTV values for ^{134}Cs and ^{137}Cs obtained in the Fukushima Daiichi region.

	Type of surface	PTV ^{134}Cs	PTV ^{137}Cs
Location 1, May 2013	Grit	13.7	9.9
Location 1, November 2014	Grit	14.0	10.3
Location 2, May 2013	Sand	20.2	10.7
Location 2, November 2014	Sand	18.9	10.7
Location 3, May 2013	Asphalt	23.7	11.5
Location 4, May 2013	Grass	18.1	10.1
Location 4, November 2014 (after clean-up)	Open soil/Sand	9.7	5.4
Location 5, May 2013	Grit	18.3	9.9
Location 6, November 2014	Open soil	20.6	11.8
Location 7, November 2014	Sand/Grit	14.7	9.1
Location 8, November 2014	Sand	19.9	12.7

The PTV ratio uncertainties presented in Tables 2 and 3 are significant. As mentioned earlier, the PTV ratio would be reduced if the activity is located close to the edges of the field of view for measurements in Table 3. This would be improved by collimation; collimating the detector to a field of view radius of 3 m would significantly reduce this effect. The collimator used outside Fukushima Daiichi exhibited a field of view >3 m and could, in practical terms, be further optimized. However, the pronounced increase in the ^{134}Cs PTV ratio at all locations (Table 2) indicates an improvement achieved already in the current constellation of the collimation. This improvement could also be ascribed the fact that the 6 m field of

view in radius is well adapted to limit the prolate scatter volume to intersect with the ground.

The perturbation of the ^{137}Cs PTV ratio by ^{134}Cs originates from primary photons undergoing Compton scattering between the source and the detector, and was detected in the ^{137}Cs valley. In the case of fallout, the ratio between ^{134}Cs and ^{137}Cs when measuring the PTV ratio pulse height distribution can almost immediately reveal whether the ^{137}Cs PTV ratio is usable. The investigations in Paper IV showed perturbations in the ^{137}Cs PTV ratio for of ^{134}Cs:^{137}Cs activity ratios down to 1:100. This was much lower than intuitively expected but considered reasonable in retrospect. The probability of a scattered photon being registered in the valley is lower than the probability of being registered further down in the Compton pulse height distribution. This will unfortunately result in significantly high valley counts from a gamma line further up in the pulse height distribution, even if the deposition amount in combination with yield is less than that of ^{137}Cs. The *in situ* measurements in Japan ranged over approximately 2.5 years, and the ^{134}Cs:^{137}Cs activity ratio changed during this time period from 1:2 to 1:4.5. This would decrease the perturbation and increase the PTV ratio up to 30%. However, the downward migration in the ground during the same period of time decreases the PTV ratio. Results obtained in Sweden approximately a decade after the Chernobyl accident, shows a migration rate of a few millimeters a year (Isaksson and Erlandsson, 1998b; Isaksson et al., 2001). This would only result in a marginal decrease in the PTV ratio. When evaluating the observations made at the same locations on different occasions, there was no significant change in the PTV ratio that can be ascribed to the aforementioned processes (see locations 1 and 2 in Table 3).

The compensation for the valley background presented in Paper II (Eq. 2 and Section 1.3.2) was utilized in this study and offered a simpler method for use with a single full energy peak pulse height distribution. The focus in this thesis was to find field operative solutions to challenges identified in the use of the PTV method. Using a background valley ROI to the right of the peak has been one way of meeting these challenges. Of course, there are drawbacks with all methods of compensating for the background counts in the valley ROI. The more complex method, i.e., natural background stripping or background slope estimation, will complicate calculations for estimating the number of net pulses in the valley. A third option is to relate the number of background pulses to the peak count-rate of the perturbing radionuclide. However, this requires a pre-assumption of the depth distribution in the ground, for the perturbing radionuclide, and this information is rarely available.

When viewing the results from *in situ* measurements in Japan, there is clear evidence of pulse summation. How this affects the PTV ratios of the cesium radionuclides will need to be investigated further. One plausible assumption would be that the summed pulses are evenly distributed over the pulse height distribution and the slopes in the

valley and background valley ROI are equally affected. However, this effect adds uncertainty to the PTV ratios obtained *in situ*, as the number of pulses in the background increases while the number of net counts in the valley remain the same.

4 General discussion

This work has investigated methods to transform measured ^{137}Cs "surface deposition" to a true mean deposition (Bq/m^2) and to derive a depth distribution-dependent coefficient from the ^{137}Cs PTV ratio obtained by *in situ* measurement. The work has also focused on finding an optimal size and field of view for an HPGe detector under field conditions. The estimated burial depth for the $^{134, 137}$Cs radionuclides in the ground is useful information when calculating the total activity, and use of the PTV ratio could possibly increase the accuracy in that estimate. It is also valuable information for decision makers in order to provide more accurate answers to strategic questions raised by the authorities and the public.

The investigation of the PTV ratio at different incident angles and different point source burial depths clearly showed that there is an area underneath the detector that provides information on shallow or no source burial depths with high sensitivity. The area is subtended by the angle interval between the areas immediately underneath the detector and to where the prolate volume intersects with the ground. This area can be actively selected by collimation of the detector field of view in order to enhance the possibility of extracting more accurate estimates of the deposition. The collimation will exclude incident angles where the correlation between valley and peak may be lost due to ground penetration of the deposition. When collimating the detector *in situ* in Fukushima Daiichi (Japan) partly following the recommendations of Paper III and limiting the detector field of view radius to approximately 6 m, the ^{134}Cs PTV ratio increased. The ^{137}Cs PTV ratio did not follow the same trend, however. Several explanations can be considered, but the main reason is that scattered photons from higher energies in the pulse height distribution interfere with the ^{137}Cs PTV ratio.

It is difficult to compare the ^{137}Cs PTV ratios for an unshielded detector in Paper IV to previously published results, as earlier measurements were made under non-optimized circumstances in which the incident angles were too large. At larger distances (>15-20 m) *in situ,* it is likely that almost no photons scattered in the ground will reach the detector, except for the ones originating from scatter in the soil surface. This effect was observed in Paper II (Figure 22). The point sources measured at the ground surface tend to have an increased PTV ratio with increasing distance, which is a verification of the above statement and absent in previous studies (Zombori et al., 1992; Gering et al., 1998; Hjerpe et al., 2002; Kastlander et al., 2005). The ^{137}Cs PTV ratio of these measurements would most likely consist of a subset of

unrelated peak and valley photons (i.e., they originate from different parts of the deposition). This means that incident angles from a surface-distributed deposition could contribute to the PTV ratio very differently with increasing radius from the detector. Furthermore, the ^{137}Cs PTV ratio will change between surface segments at different distances from the detector, and the obtained PTV ratio will be a weighted mean of all contributing distances. One major conclusion from the work is that there should be marginal loss of scattered photons in the ground in order to maintain the sensitivity of shallow burial depths in the PTV ratio.

Each detector is an individual entity and has to be properly investigated beyond normal calibration procedures for *in situ* measurements in order to be useful as a ^{137}Cs PTV ratio detector. One interesting conclusion is that, even though a detector is to be investigated individually, the results indicate that coaxial HPGe detectors are usable independent of size and type, i.e., regardless of whether it is a p- or n-type detector (Figure 4, Paper III). Furthermore, using a 30 keV, instead of a 20 keV, valley ROI results in similar PTV ratios between the detectors (Table 1), allowing the choice of optimal rel. efficiency for each measurement situation. It is unclear if choosing a 30 keV valley ROI in situations like Georgia was the correct decision. It is clear, however, that a wider valley ROI increases the possibility of perturbations by other miscellaneous radionuclides that are present, since the 30 keV valley ROI is more easily perturbed by full energy peaks or Compton edges compared to a 20 keV valley. The choice of valley range is dependent on the measurement situation and it is up to the user to make that choice.

The perturbation of a PTV ratio from higher photon energies that contributes scattered photons in the valley has to be compensated. In the case of reactor fallout, the ^{134}Cs PTV ratio can be used as a substitute for^{137}Cs during the first decade after the accident. The perturbation of the ^{137}Cs valley caused by ^{134}Cs Compton scattered photons was significant when performing PTV measurements in Fukushima Daiichi. The ^{137}Cs PTV ratio was below reasonable values compared to soil sampling results. The change in the ^{134}Cs PTV ratio due to collimation enabled the use of the PTV method and more accurate estimation of the cesium burial depth. The usability of the PTV method is still questionable for areas with high concentrations of fallout or when under the influence of other radionuclides. However, there are several ways to investigate and improve the PTV method further (see Section 4 in Paper IV).

The Monte Carlo calculations showed that modeling the detector in as detailed a manner as possible is a helpful tool for understanding the influence of the detector components. The absolute values of the peak and valley did not match perfectly between simulations and measurements for all simulated situations under the best achievable circumstances. The conclusion is that simulations cannot fully replace measurements in specific applications, such as the PTV method.

The 123% rel. efficiency HPGe detector in a backpack configuration, as used in Georgia, has a higher sensitivity than $LaBr_3$ and NaI(Tl), both 76.2 mm (Ø) by 76.2 mm in size, regardless of the inferior photon interaction cross section of germanium. However, in the terms of field operations, the HPGe detector system is more cumbersome to use than the scintillator system. The EBS in tasks of this kind should be further developed to enable fast and efficient production of high-quality results in demanding situations. How to generically compensate for intense higher photon energies in the pulse height distribution, whether they originate from fallout or a high activity source, has not yet been solved. When estimating the point source depth affected by the aforementioned higher energy gamma radiation, there are tools the operator can use to increase the accuracy of the PTV ratio. One can look at the ratio between the gross valley count and the background ROI to the right of the full energy peak. If the ratio has a value close to 1, the statistical uncertainty in the ^{137}Cs PTV ratio is too large.

The detector electronics, detector specifications, and other details in the geometry of the detector and its surroundings, are still important factors when determining the PTV ratio. Furthermore, the inhomogeneity in the deposited fallout on the ground, the composition of radionuclides, and the intensity of the photon field are thought to be the major factors affecting cesium PTV ratios. These factors lead to large uncertainties in the surveys conducted in this thesis and need to be addressed in the future. The proposed methodology in section 5.2 is a tentative suggestion and an important outcome of this thesis.

5. Outlook and limitations

5.1 Limitations of this work

One limitation of the work done in this thesis is that a PTV ratio has not been calculated or measured in a fully controlled setup for a surface source. The $^{134, 137}$Cs PTV ratios measured outside Fukushima Daiichi were obtained without exact knowledge of the source or the spatial distribution and can only serve as an indication. The PTV results are not valid for detectors other than the coaxial type of HPGe detectors. No more knowledge is available on the content of the repository in Georgia than the information obtained by measurements on site. This is a usual limitation when performing emergency preparedness measurements in general, i.e., the measurement situation is not fully documented and not always under control. The analysis of the statistical uncertainty presented in 2.3 is only valid for the measurements made in the LBC room but can serve as an indicator for other similar situations. The effects on the pulse height distribution of summation in high-intensity radiation fields *in situ* were not investigated in this thesis.

5.2 Suggested PTV methodology

Based on the outcome of the studies in this thesis, a suggestion for how to use the PTV method implementing the new knowledge is presented below. The following suggestions can be seen as a guide rather than a specific method and will require the operator's own judgment.

1. Decide the valley ROI range and position in terms of photon energy, and choose the measurement height of the detector.
2. For a given detector, investigate the maximum PTV ratio corresponding to the incident angle according to Paper III. *This will provide the internal valley background of the detector.*

3. Investigate what maximum source intensity (i.e., detector dead time) is usable. *Use the background ROI counts as an indicator of when summation starts to occur, presenting undesired summed pulses in the background ROI.*

4. Choose a location with representative background. Perform a PTV ratio measurement at this representative location that is virtually unaffected by fresh fallout. Determine the valley count rate in relation to measured live time. *From this measurement, determine the ratio between the selected background ROI and valley ROI. This will include the historic fallout of ^{137}Cs, which is unrelated to the fresh fallout.*

5. Apply a collimator with proper specifications to the detector to limit the field of view. *The detector field of view should not allow surface-distributed source photons to interact with the ground surface, and produce detectable valley photons in the ground. This means in practical terms that the photon path with a maximum scatter angle (corresponding to the lower limit of the valley ROI) should not intersect with the ground.*

6. Investigate the contribution from the collimator itself in a low background environment. *Estimate the contribution by comparing the differences between collimated measurements and the measurements in point 2 above for incident angles between 0° and 90°.*

7. Investigate the PTV ratio with thin point sources between 0° and 90°, with the source on the ground surface and with source burial depths relevant to the application, this within the chosen collimator angles according to Paper III. *When using HPGe detectors of a similar nature as in Table 1, the operator could consider using the results in Paper III.*

8. Subtract all of the internal (measurement system) contributions (obtained in points 4 and 6 above) from the valley counts obtained in point 7. *Subtract the estimated contribution of the background in relation to the live time measurement.*

9. Perform integration over the angles between 0° and 90° and calculate the PTV ratio for the different penetration depths and the data obtained in point 8.

10. Present the PTV ratio as a function of depth, indicating the penetration depth (i.e., mean mass depth of the cesium radionuclide deposition).

5.3 Outlook and scope for future studies

The thesis is the product of working part time in research and part time in practical emergency preparedness work and planning. This has given me an opportunity to implement the results of my research in my emergency preparedness work, field expeditions, education and other emergency tasks. This has also given me the opportunities for discussions with others over time and a unique opportunity to build contacts with colleagues around the world.

For future development, additional work needs to focus on designing a collimator that provides:

i) Sufficient suppression of incident angles beyond 3.0 m (measurement height 1 m),

ii) Minimal scatter with energies in the selected valley range originating from the collimator.

A method has to be developed to determine the mean mass depth from collimated measurements. In addition, further investigations concerning calculation of the PTV ratio originating from the area underneath the detector defined by the collimator have to be performed. Representative PTV ratios need to be obtained *in situ* with collimation, including different ground materials with various moist content and different source energies for a variety of HPGe detectors, including coaxial and others.

The use of Monte Carlo calculations in relation to PTV ratios needs to be further developed. Calibration measurements need to be replaced over time with simulated calibrations. A focus on understanding the perturbing factors and uncertainties would be a natural and important part of future work. Difficulties matching the efficiency between measurements and simulations are a prominent problem that mitigates the development of models for future calculations and understanding.

The use of gamma lines with photon energies >662 keV and the combined energies of 796 and 802 keV (^{137}Cs and ^{134}Cs) to assess PTV ratio and depth in other situations are interesting. This would not only provide more understanding of the possibilities of the PTV method, but also complement other applications, such as the decommissioning of radioactive waste, especially with the use of collimators.

When estimating point source depths in situations like in Georgia, the PTV ratio could perhaps be utilized to describe the burial depth of ^{60}Co sources with higher gamma energies. The situation differs from fallout and estimating burial depth, as the higher energy is perhaps better suited for those burial depths. This needs to be investigated further because it could improve estimation of the position of sources in situations such as the decommissioning of nuclear facilities.

6. Acknowledgments

Thanks to:

My Supervisors:

To all of you for the scientific advice and the discussions where we had so much fun.

Christer for being a good friend, giving me the opportunity to do fun research, and for successfully guiding me to where I am today.

Christopher for just sharing a different perspective of a lot of things and your great care for details.

Sören for your endless optimism, always sharing your time when you don't have any to spare, and for the guidance on what to do when something goes south…

My mentor:

Robert Finck. You always have the time to talk and listen to discoveries and all the crazy thoughts. I will always remember your two well-meant and inspiring sentences:

"*You are not an ordinary PhD student*" and "*Collimators are shit! If you make it work I will change my mind*".

My Co-authors:

Jonas Nilsson for your positive attitude to solve problems and that I always could count on your help no matter what.

Joakim Söderberg for the friendship and the possibility to do things together that few others have done.

My colleagues in the environmental radiology group:

Therése, Christian and Mattias, for your friendship, support and taking the time to discuss and just listen.

My other colleagues at Lund University, and Malmö and Lund University Hospital.

My professor Lars E Olsson, Martin, Vivéca, Hannie, Lars, Daniel, Magnus, Maria, Lena, Lovisa, Emilie, Simon, Sara B, Kai, Cecilia, Hanna Anja, Anders T., and really everybody.

My former colleagues:

Jonas Jarneborn for your help during field trips, exercises to collect data and for your help with the graphics.

Ünal Ören for friendship and good advice.

Marcus Persson for your help during field work.

My co-workers in the area of radiation protection and emergency preparedness:

Simon Karlsson, Peder Kock, Jonas Boson, Olof Karlberg and Jan Johansson and everybody else at SSM for always setting time aside to support, helping out and allowing me to be part of all the fun! You are great!

Karin Lindh, Pelle Postgård and Torbjörn Nylén, and all participants in the NESA group, for your interest and inspiration of my work.

Stefan and Stefan at Gammadata for your help with detectors and tricky questions.

Patrick Kenny at IAEA, for being flexible and arranging the possibilities to do research measurements in Fukushima, Japan.

Rodolfo Gurriaran at IRSN, for the help with Figures, discussions and interesting literature difficult to find online.

My friend

Mr. Minoru Takeishi, Fukushima Environmental Safety Center, JAEA, for your support and for discussions regarding the JAEA measurements and the results obtained in the Fukushima region. This has meant the world to me.

Japan

Thanks to the country of Japan, who invites and supports foreign authorities and scientists to learn from the tragic accident in Fukushima.

Family

My parents, brother, friends and relatives who perhaps didn't understand what I was talking about but still cared to listen and comment.

Sweden

The country and Government, for trusting me with the responsibility of finding new facts through research.

All of my other colleagues and friends in Sweden and the world that has contributed to this thesis in one way or another. No one should feel left out.

7. Bibliography

Abramenkovs, A., 2006. Upgrading of Radon-type near surface repository in Latvia, in: Proc. TOPSEAL2006, Olkiloto 17.9-20.9 2006 Finland. Hazardous wastes management state agency, Ministry of Environment, 31 Miera Street, Salaspils, LV-2169, Latvia Retrieved Apr. 4, 2013: http://www.euronuclear.org/events/topseal/transactions/Paper-Poster-Abramenkovs.pdf

Baeza, A., Corbacho, J.A., 2010. *In situ* determination of low-level concentrations of ^{137}Cs in soils. Appl. Radiat. Isot. 68, 812-815.

Beck, H.L., Decampo, J., Gogolak, C., 1972. *In situ* Ge(Li) and NaI(Tl) gamma-ray spectrometry. HASL-258. United States Atomic Energy Commission, Health and Safety (TID-4500) , 75 p., 75.

Boson, J., Plambäck, A., H., Ramebäck, H., Ågren, G., Johansson, L., 2009. Evaluation of Monte Carlo-based calibrations of HPGe detectors for *in situ* gamma-ray spectrometry, J Environ Radioactiv 100, (11), 935–940

Buzulukov, Y .P., Dobrynin, Y.L., Release of radionuclides during the Chernobyl accident. In: The Chernobyl Papers, Vol 1, Doses to the Soviet Population and Early Health Effects Studies, (Ed by S.E.Merwin and M.I.Balonov), Research Enterprises, Washington; pp 3-21; 1993

Cresswell, A., J., Sanderson D.C.W., 2012. Evaluating airborne and ground based gamma spectrometry methods for detecting particulate radioactivity in the environment: a case study of Irish Sea beaches. Sci. Tot. Environ. 437, 285-296. doi:10.1016/j.scitotenv.2012.08.064.

Edvardsson, K., External doses in Sweden after the Chernobyl fallout, In: The Chernobyl Fallout in Sweden. Results from a research programme on environmental radiology, (Ed by Leif Moberg), the Swedish Radiation Protection Institute, Stockholm, Sweden, pp 527-545; 1991.

Finck, R., R., 1992. High resolution field gamma spectrometry and its application to problems in environmental radiology (Doctoral dissertation). Departments of Radiation Physics, Lund and Malmö; Malmö, Sweden.

FOA C40324, Varning och rapportering vid radioaktivt nedfall från kärnvapen, Krigsorganisation på fredens grund. Ulvsand, T., Finck, R., Edvardsson, K., Larsson, T., Perrson, G., Report No. C40324-4.3, 1994, ISSN 0347-2124

Fulöp M, Ragan P, 1997. In-situ measurements of ^{137}Cs in soil by unfolding method. Health Phys 72:923–930

Gering, F., Hillmann, U., Jacob, P., & Fehrenbacher, G., 1998. *In situ* gamma-spectrometry several years after deposition of radiocesium. Part II. Peak-to-valley method. *Radiation Environmental Biophysics,* 37(4), 283–291.

Gilmore, G. R., Practical Gamma-ray Spectroscopy 2nd edition, 2008, Print ISBN: 9780470861967.

Heaps, Leo, 1978. *Operation Morning Light : Terror in our Skies : The True Story of Cosmos 954*. New York: Paddington Press Ltd. ISBN 0-7092-0323-3.

Hjerpe, T., & Samuelsson, C., 2002. Accounting for the depth distribution of ^{137}Cs in on-line mobile gamma spectrometry through primary and forward-scattered photons. *Radiation and environmental biophysics*, *41*(3), 225–230.

Hillmann U, Schimmack W, Jacob P, Bunzl K, 1996. In situ γ-spectrometry several years after deposition of radiocesium. I. Approximation of depth distribution by the Lorenz function. Radiat Environ Biophys 35:297–303.

ICRU Report 53, , *International Commission on Radiation Units and Measurements,* Gamma-ray Spectrometry in the Environment, Report No. 53, 1994.

International Atomic Energy Agency (IAEA), "The radiological accident in Goiânia", tech. rep., Vienna, Austria, 1988. ISBN 92-0-129088-8.

International Atomic Energy Agency (IAEA), "The radiological accident in Lia, Georgia", tech. rep., Vienna, Austria, Dec 2014. ISBN 978-92-0-103614-8.

Isaksson, M., Erlandsson, B., 1998b. Models for the vertical migration of 137Cs in the ground, a field study. J. Environ. Radioact. 41, 163–182.

Isaksson, M., Erlandsson B., Mattsson, S., 2001. A 10-year study of the ^{137}Cs distribution in soil and a comparison of Cs soil inventory with precipitation-determined deposition. J. Environ. Radioact. 55, 47-59.

Isaksson, M., Rääf, C.L., 2016. Environmental Radioactivity and Emergency Preparedness,. ISBN: 978-1-4822-4464-9.

Kastlander, J., Bargholtz, C. 2005. Efficient *in situ* method to determine radionuclide concentration in soil. Nucl. Instrum. Meth. A. 547(2-3), 400–410.

Karlberg, O., 1990. *In situ* gamma spectrometry of Chernobyl fallout on urban and rural surfaces, evaluation of different methods to estimate the deposited activity on surfaces with rough structures. Report Studsvik NP-89/108, Studsvik Nuclear Nyköping, Sweden.

Kock, P., Samuelsson, C., 2007. Monte Carlo Simuleringar av framåtspridd Compton-strålning från radionuklider i mark. MSc thesis, Med. Rad. Physics Dept. Lund, Lund University.

Lemercier, M. Dévelopment d'une méthode analytique pour quantifier par spectrométrie gamma in-situ les radionucléides présents dans les sols (Doctoral Dissertation), 2008. Labroratorie de Mesure de la Radioactivité dans l'Environnement (IRSN), IRSN/IRSN-2008/94.

Lidström, K., Nylén, T., 1998. Beredskapsmetoder för mätning av radioaktivt nedfall. FOA report nr. FOA-R-98-00956-861-SE (in Swedish).

Los Alamos Monte Carlo Group, "MCNP-A General Monte Carlo N-Particle Transport Code Version 5," https://mcnp.lanl.gov/mcnp5.shtml

Marzocchi, O., Breustedt, B., Urban, M., 2010. Characterisation, modelling and optimisation of the model of a HPGe detector with the aid of point sources. Appl. Radiat. Isot. 68, 1438-1440.

Milbrath BD, RC Runkle, TW Hossbach, WR Kaye, EA Lepel, BS McDonald, and LE Smith, 2005b. Characterization of alpha contamination in lanthanum trichloride scintillators using coincidence measurements. Nuc. Inst. and Meth. A, vol. 547, pp. 504-510.

Mosey, D., Reactor Accidents. Nuclear Safety and the Role of Institutional Failure, Nuclear Engineering International Special Publications; 1990.

Nisbet, AF., Brown, J., Howard, BJ., Beresford, NA., 2010. Decision aiding handbooks for managing contaminated food production systems, drinking water and inhabited areas in Europe. Radioprotection, 45, S23-S37.

Nisbet, AF., Chen, SY., 2015a. Decision making for late-phase recovery from nuclear or radiological incidents: new guidance from NCRP. Annals of the ICRP Volume 44, No. 1S, 162-171.

Nisbet A., S Watson, S., Brown, J., 2015b. UK Recovery Handbooks for Radiation Incidents 2015 Version 4. PHE-CRCE-018. www.gov.uk/government/publications/uk-recovery-handbooks-for-radiation-incidents-2015

Panza, F. Dévelopment de la spectrométrie gamma *in situ* pour la carthographie de site (Doctoral Dissertation), 2012. Labroratorie de Mesure de la Radioactivité dans l'Environnement, (LMRE, IRSN), PRP-ENV/STEME/LRME-2012-016.

Radiakskyddsberedskap 2000, 1998. Räddningsverket Karlstad. ISBN: 91-88891-34-8

Saito, K., Tanihata, I., Fujiwara, M., Saito, T., Shimoura, S.,Otsuka, T., Onda, Y., Hoshi, M., Ikeuchi, Y., Takahashi, F., Kinouchi, N., Saegusa, J., Seki, A., Takemiya, H., Shibata, T., 2015. Detailed deposition density maps constructed by large-scale soil sampling for gamma ray emitting radioactive nuclides from the Fukushima Dai-ichi Nuclear Power Plant accident. J Environ Radioactiv, 139, 308-319.

Thummerer S., Jacob P., 1998, Determination of depth distributions of natural radionuclides with *in situ* gamma spectrometry, Nucl. Instrum. Meth. A416(1), 161-178.

Tyler, A.N., Sanderson, D.C.W., Scott, E.M., 1996. Estimating and accounting for ^{137}Cs source burial through *In-situ* gamma spectrometry in salt marsh environments. J Environ Radioactiv, 33, (3), 195–212

Tyler, A.N., 1999. Monitoring anthropogenic radioactivity in salt marsh environments through in situ gamma-ray spectrometry. J. Environ. Radioact. 45, 235–252.

Tyler, A.N., 2004. High accuracy in situ radiometric mapping. J. Environ. Radioact. 72, 195–202.

UNSCEAR, 1988. Report to General Assembly, with Scientific Annexes and Appendix: Acute radiation effects in victims of the Chernobyl nuclear power plant accident, United Nations, New York.

UNSCEAR, 2000. Sources and Effects of Ionizing Radiation. Report to General Assembly, with Scientific Annexes, United Nations, New York.

UNSCEAR, 2013. Report to General Assembly, with Scientific Annex A, Levels and effects of radiation exposure due to the nuclear accident after the 2011 great east Japan earthquake and tsunami, United Nations, New York.

Yoschenko, V.I., Kashparov, V.A, Protsak, V.P., Lundin, S.M., Levchuk, S.E., Kadygrib, A.M, Zvarich, S.I., Khomutinin, Yu.V., Maloshtan, I.M., Lanshin, V.P., Kovtun, M.V., Tschiersch, J., 2006. Resuspension and redistribution of radionuclides during grassland and forest fires in the Chernobyl exclusion zone: part I. Fire experiments. J. of Environ. Rad. 86(2), 143-163.

Yoshida, N., Takahashi, Y., 2012. Land-surface contamination by radionuclides from the Fukushima Daiichi nuclear power plant accident, Elements 8 3, 201–206.

Zombori, P., Andrasi, A., Nemeth, A., 1992. I*n-situ* gamma spectrometric measurement of the contamination in some selected settlements of Byelorussia (BSSR), Ukraine (UkrSSR) and the Russian Federation. J Environ Radioactiv, 17, 97-106.

Zombori, P., Andrasi, A., Nemeth, A., 1992b. A new method for determination of radionuclide distribution in the soil by *in situ* gamma-ray spectrometry. *Report KFKI-1992-20/K,* Hungarian Academy of Sciences, Central Research Institute for Physics, Budapest.

Printed by Media-Tryck, Lund 2017 NORDIC ECOLABEL, 3041 0903

LUND UNIVERSITY

Faculty of Science Doctoral Dissertation Series
Medical Radiation Physics, Malmö
ISBN 978-91-7753-240-8